

## Vaccine Development

How to cite:

International Edition: doi.org/10.1002/anie.202009663

German Edition: doi.org/10.1002/ange.202009663

## Overcoming Symmetry Mismatch in Vaccine Nanoassembly through Spontaneous Amidation

Rolle Rahikainen<sup>+</sup>, Pramila Rijal<sup>+</sup>, Tiong Kit Tan<sup>+</sup>, Hung-Jen Wu, Anne-Marie C. Andersson, Jordan R. Barrett, Thomas A. Bowden, Simon J. Draper, Alain R. Townsend,\* and Mark Howarth\*

**Abstract:** Matching of symmetry at interfaces is a fundamental obstacle in molecular assembly. Virus-like particles (VLPs) are important vaccine platforms against pathogenic threats, including Covid-19. However, symmetry mismatch can prohibit vaccine nanoassembly. We established an approach for coupling VLPs to diverse antigen symmetries. SpyCatcher003 enabled efficient VLP conjugation and extreme thermal resilience. Many people had pre-existing antibodies to SpyTag:SpyCatcher but less to the 003 variants. We coupled the computer-designed VLP not only to monomers (SARS-CoV-2) but also to cyclic dimers (Newcastle disease, Lyme disease), trimers (influenza hemagglutinins), and tetramers (influenza neuraminidases). Even an antigen with dihedral symmetry could be displayed. For the global challenge of influenza, SpyTag-mediated display of trimer and tetramer antigens strongly induced neutralizing antibodies. SpyCatcher003 conjugation enables nanodisplay of diverse symmetries towards generation of potent vaccines.

## Introduction

As nanostructures grow and develop, there are often mismatches in size and symmetry at interfaces, including for crystal lattices,<sup>[1]</sup> metal-organic frameworks<sup>[2]</sup> and natural biological assemblies.<sup>[3]</sup> For example, Adenovirus has trimeric fibers extending from a capsid vertex with C5 (5-fold cyclic) symmetry, while Salmonella's injectisome has a C24 inner ring connecting to a C15 outer ring.<sup>[3]</sup> Artificial protein nanostructures have shown great potential for therapy,<sup>[4]</sup> energy harvesting<sup>[5]</sup> and vaccines for global health,<sup>[6,7]</sup> so it is important to establish approaches to overcome symmetry mismatch. Vaccines based on purified protein antigens generally have excellent safety profiles, while their facile

manufacturing allows rapid response to antigenic variation and emerging pandemic threats.<sup>[8]</sup> However, such protein antigens show mediocre immunogenicity unless displayed on virus-like particles (VLPs).<sup>[8]</sup> VLP-display facilitates antigen drainage to lymph nodes, complement activation, uptake by antigen-presenting cells, and B cell receptor crosslinking.<sup>[8]</sup> However, genetic fusion of antigens to VLP subunits is hindered by different requirements for folding and post-translational modifications, as well as symmetry mismatches.<sup>[9]</sup>

Modular assembly of antigen-decorated VLPs through SpyTag/SpyCatcher technology represents an alternative avenue.<sup>[9]</sup> SpyCatcher is a 12 kDa protein that we previously engineered to form a spontaneous amide bond to its peptide partner SpyTag (Figure 1A).<sup>[10]</sup> While the display of monomeric antigens using modular ligation (Figure 1B) is established,<sup>[11–13]</sup> there has been no systematic study of the display of antigens possessing different cyclic or dihedral symmetries (Figure 1C). However, a large fraction of clinically important antigens are multimeric, including surface proteins from influenza, Ebola virus and coronaviruses.<sup>[6–8]</sup> Potential challenges for VLP-display of multimeric antigens include unpredictable antigen density on the VLP, antigen instability, or VLP crosslinking leading to aggregation (Figure 1D).

Here, we establish a VLP showing efficient production, quantitative amide bond formation, and extreme resilience. We characterize VLP reactivity with multimeric antigens of diverse symmetry, spanning a range of important human and veterinary pathogens. The level of pre-existing human immunity against different SpyTag/SpyCatcher generations is investigated using serum from healthy donors. Finally, we establish the new platform to overcome the obstacle of display of both trimeric and tetrameric influenza antigens, enabling induction of potent neutralizing antibody responses.

[\*] R. Rahikainen,<sup>[†]</sup> H.-J. Wu, A.-M. C. Andersson, M. HowarthDepartment of Biochemistry, University of Oxford  
South Parks Road, Oxford, OX1 3QU (UK)  
E-mail: mark.howarth@bioch.ox.ac.ukP. Rijal,<sup>[†]</sup> T. K. Tan,<sup>[†]</sup> A. R. Townsend  
MRC Human Immunology Unit, MRC Weatherall Institute of  
Molecular Medicine, Radcliffe Department of Medicine  
University of Oxford, Oxford, OX3 9DS (UK)  
E-mail: alain.townsend@imm.ox.ac.ukA.-M. C. Andersson  
Current address: InProTher Aps  
Ole Maaløes Vej 3, 2200 København (Denmark)J. R. Barrett, S. J. Draper  
Jenner Institute, University of Oxford, Oxford, OX3 7DQ (UK)

T. A. Bowden

Wellcome Trust Centre for Human Genetics  
University of Oxford, Oxford, OX3 7BN (UK)

[†] These authors contributed equally to this work.

Supporting information and the ORCID identification number(s) for the author(s) of this article can be found under:  
<https://doi.org/10.1002/anie.202009663>.

© 2020 The Authors. Published by Wiley-VCH GmbH. This is an open access article under the terms of the Creative Commons Attribution License, which permits use, distribution and reproduction in any medium, provided the original work is properly cited.

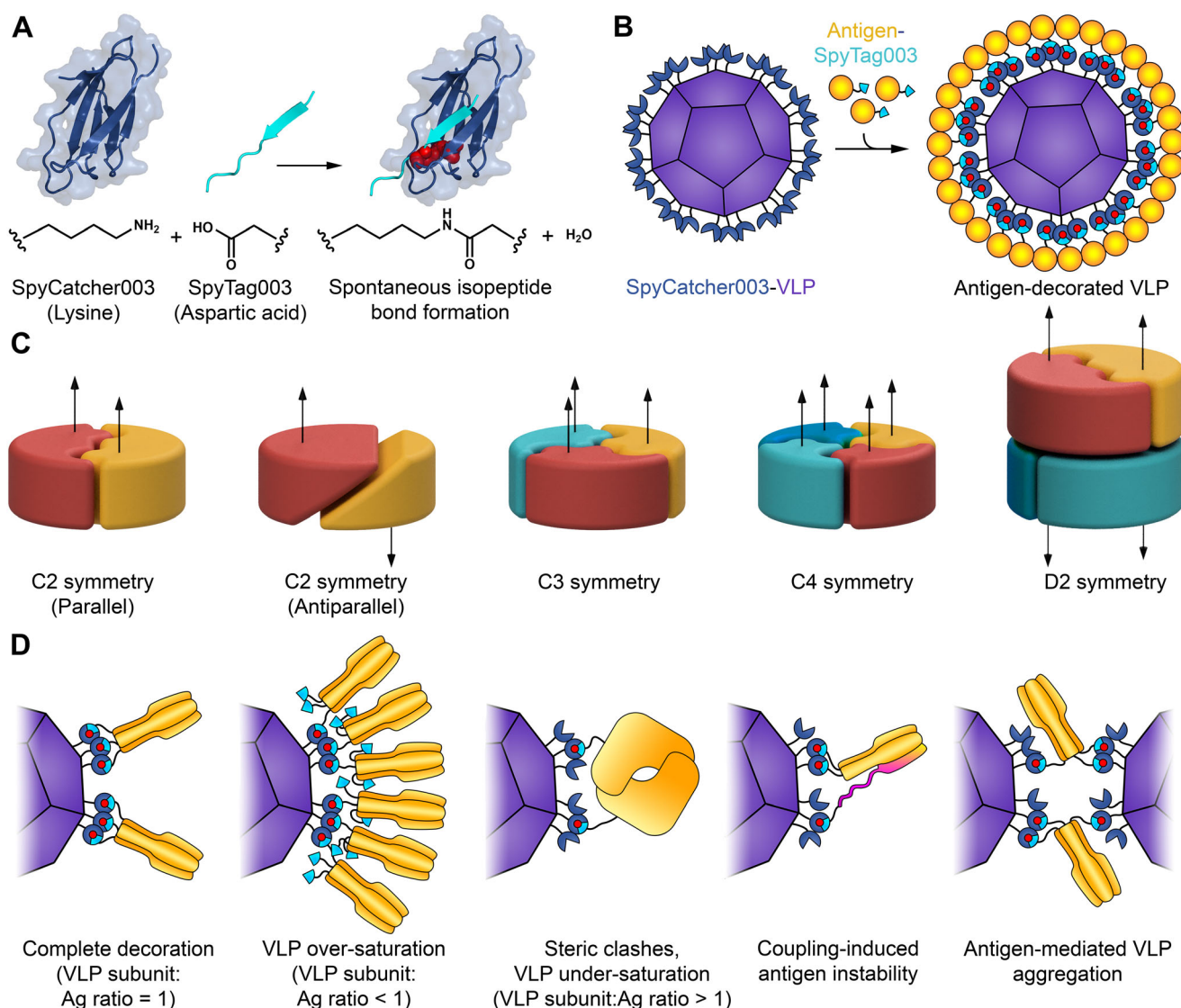


**Figure 1.** Spy-nanoassembly for different antigen symmetries. A) Schematic of reactive protein/peptide pair. Lysine on SpyCatcher003 (dark blue) forms a spontaneous amide bond with aspartic acid of SpyTag003 (cyan). Residues forming the isopeptide bond are colored as red spheres, based on PDB ID: 4MLI. B) Plug-and-display vaccine assembly. Genetic fusion of a monomeric antigen (yellow) to SpyTag003 (cyan) allows simple efficient reaction (isopeptide bond in red) on nanoparticles (purple) fused to SpyCatcher003 (dark blue). For clarity, only a portion of SpyCatcher003 sites are shown. C) Typical symmetries of multimeric protein antigens (arrow indicates relative subunit orientation). D) Matching of nanoparticle and antigen symmetry. VLP-display of multimeric antigen (in orange) may proceed to different display densities. Coupling of multimeric antigens could destabilize the antigen (misfolding in magenta) or bridge VLPs, leading to aggregation.

## Results

Initially we established an optimal nanoparticle scaffold for vaccine assembly. The Baker laboratory designed a dimeric interface into the trimeric aldolase from the thermophilic bacterium *Thermotoga maritima*, leading to porous 60-mer dodecahedra.<sup>[14]</sup> We previously increased the resilience and modular reactivity of these particles to generate SpyCatcher-mi3.<sup>[15]</sup> In parallel, we recently developed SpyTag003/SpyCatcher003, with reaction rate near the diffusion limit.<sup>[16]</sup> Therefore, we solubly expressed SpyCatcher003-mi3 VLPs in the *Escherichia coli* cytoplasm to high yield and investigated their biophysical and biochemical properties. The original SpyCatcher-mi3 was purified using C-tag affinity chromatog-

raphy. Since affinity-based purification increases cost and slows scaling,<sup>[17]</sup> we established affinity resin-independent purification. Combining ammonium sulfate precipitation and size exclusion chromatography (SEC) allowed efficient purification of SpyCatcher003-mi3 particles to high purity (Figure S1A–C). Given the great problem of the failure of the cold-chain for global vaccine usage,<sup>[18]</sup> we used thermal and freeze-thaw stability analyses as surrogate assays to assess the resilience of the new VLP platform. SpyCatcher003-mi3 maintained solubility even following 1 h incubation at 95 °C, exhibiting superior thermal resilience to the original SpyCatcher-mi3 platform (Figure 2 A). Similarly, SpyCatcher003-mi3 showed enhanced stability to freeze-thaw compared to SpyCatcher-mi3 (Figure 2B).



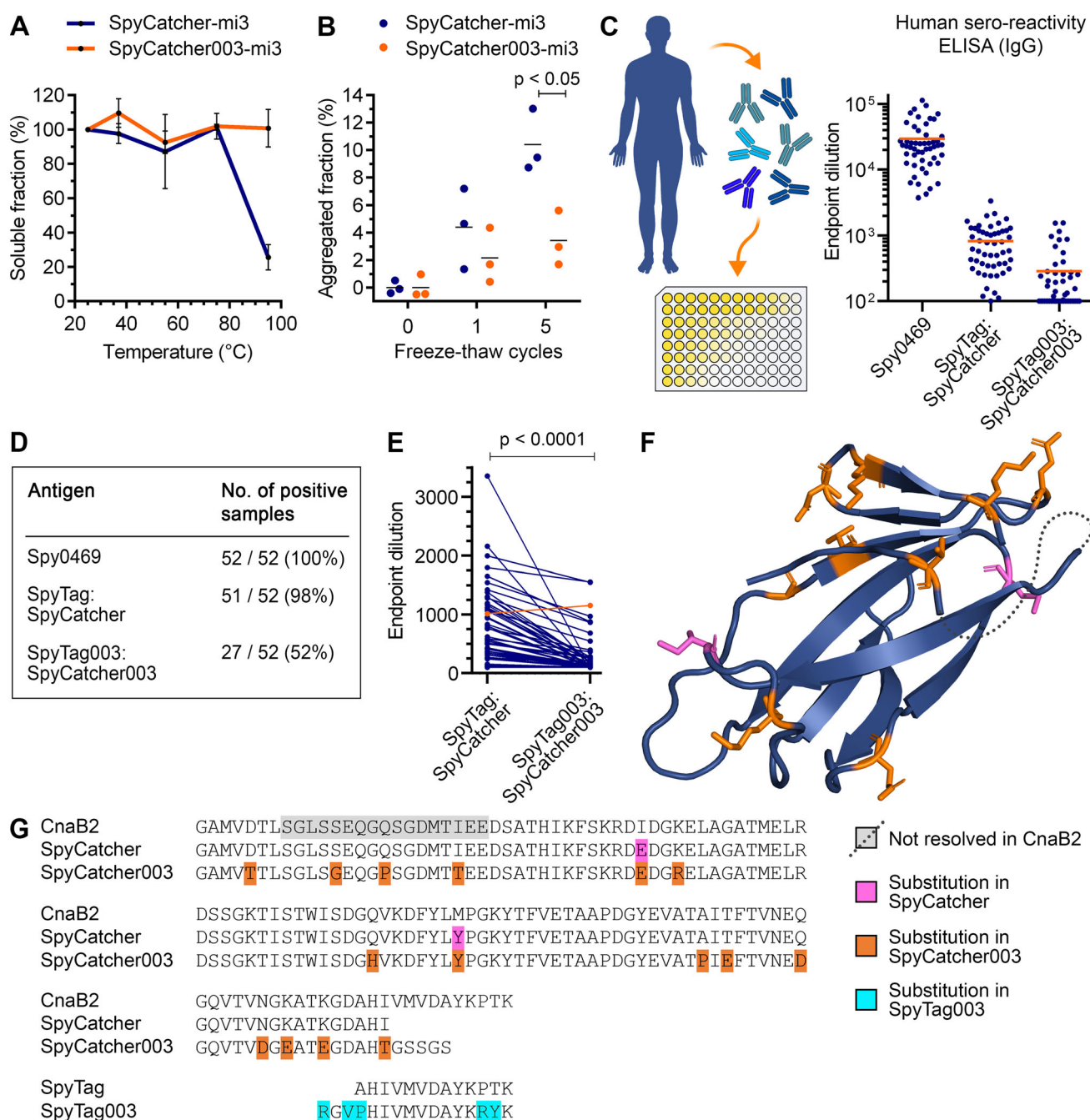


**Figure 2.** SpyCatcher003 enhanced VLP stability and decreased pre-existing sero-reactivity. A) SpyCatcher-mi3 and SpyCatcher003-mi3 were heated for 60 min at the indicated temperature, cooled to 4°C, aggregates were removed by centrifugation, and the fraction of soluble protein determined. Mean  $\pm$  s.d.,  $n=3$ . B) SpyCatcher-mi3 or SpyCatcher003-mi3 were subjected to the indicated number of freeze-thaw cycles and the insoluble fraction was removed by centrifugation. VLP in the supernatant was analyzed by SDS-PAGE. Mean is marked by a horizontal line; two-tailed Student's  $t$ -test,  $n=3$ . C) Pre-existing sero-reactivity to *S. pyogenes* antigens. Antibody titer of serum from 52 people against the positive control Spy0469, SpyTag:SpyCatcher, or SpyTag003:SpyCatcher003. Each person is shown as a dot, with the mean in orange. D) Summary of immune responses in (C). E) Pairwise comparison of titer. The person with increased titer against SpyTag003:SpyCatcher003 is indicated in orange (Wilcoxon matched-pairs signed rank test,  $n=52$ ). F–G) Structural model (PDB ID: 2X5P) of the CnaB2 domain and sequence alignment with SpyTag/SpyCatcher pairs. Substitutions from CnaB2 are magenta (SpyCatcher) or orange (SpyCatcher003). Substitutions in SpyTag003 are cyan. The dotted line indicates a region not resolved in CnaB2.

SpyTag-mediated amidation has been tested in a range of pre-clinical vaccine models, particularly for malaria,<sup>[9]</sup> but it has not been explored to what extent people have pre-existing antibodies against SpyTag/SpyCatcher. SpyTag/SpyCatcher

was engineered from the CnaB2 domain of the FbaB adhesion protein from the common human pathogen *Streptococcus pyogenes*.<sup>[10]</sup> *S. pyogenes* causes infection in 700 million people worldwide per year.<sup>[19]</sup> FbaB is predominantly

expressed by the M3 serotype of *S. pyogenes*.<sup>[20]</sup> To better understand the implications of common exposure to *S. pyogenes* for clinical development of SpyTag/SpyCatcher-based vaccines, we used enzyme-linked immunosorbent assay (ELISA) to analyze the presence of pre-existing antibodies against SpyTag:SpyCatcher and SpyTag003:SpyCatcher003 in serum samples from 52 healthy UK adults. Each Catcher was pre-reacted with the respective Tag and purification tags were removed (Figure S2A), to mimic the conjugates present on antigen-decorated VLPs. All 52 people tested positive for antibodies against the immunodominant *S. pyogenes* surface protein Spy0469,<sup>[19]</sup> confirming the expected common exposure of people to *S. pyogenes* (Figure 2C,D, Figure S2B). Antibodies to SpyTag:SpyCatcher were detected in 98 % of samples, but only 52 % gave a positive response to SpyTag003:SpyCatcher003 (5.4-fold decrease in median titer, Figure 2C,D, Figure S2C,D). In pairwise comparison only 1/52 had higher titer against SpyTag003:SpyCatcher003 (Figure 2E). Therefore, the 18 amino acid substitutions from SpyTag:SpyCatcher to SpyTag003:SpyCatcher003<sup>[16]</sup> generally decreased detection by existing human antibodies (Figure 2F,G). We confirmed this difference using sandwich ELISA with anti-His<sub>6</sub> antibody (Figure S2E,F). We investigated if high anti-Spy0469 titer predicts high anti-SpyCatcher response. Spy0469 versus SpyTag:SpyCatcher had a Pearson correlation coefficient of 0.33 ( $p = 0.02$ ,  $n = 51$ ), indicating a weak positive relationship (Figure S2G). However, we did not find a significant correlation between the Spy0469 and SpyTag003:SpyCatcher003 titres (Pearson correlation coefficient = 0.28,  $p = 0.15$ ,  $n = 27$ ) (Figure S2H). As expected, SpyTag:SpyCatcher and SpyTag003:SpyCatcher003 titers had a statistically significant positive correlation (Pearson correlation coefficient = 0.67,  $p = 0.0001$ ,  $n = 27$ ) (Figure S2I).

We have also established SnoopTag/SnoopCatcher as an orthogonal reactive pair for spontaneous transamidation and vaccine nanoassembly<sup>[21]</sup> (Figure S3A). SnoopTag/SnoopCatcher was engineered from the RrgA adhesin of *Streptococcus pneumoniae*; up to 65 % of children and 10 % of adults are asymptomatic carriers.<sup>[22]</sup> All human sera tested positive against *S. pneumoniae* immunodominant surface protein PsaA<sup>[23]</sup> (Figure S3B,C,E,F). Only 25 % were positive against SnoopTag/SnoopCatcher (Figure S3D-F). We did not find correlation between PsaA and SnoopTag:SnoopCatcher titers (Pearson correlation coefficient = 0.15,  $p = 0.63$ ,  $n = 13$ ) (Figure S3G).

To investigate VLP-display of antigens with diverse sizes and multimeric structures, we expressed a panel of SpyTag- and SpyTag003-fused proteins (Figure 3A). As a monomer, we expressed the receptor binding domain (RBD) from SARS-CoV-2 spike (Figure 3A), a vaccine candidate for Covid-19,<sup>[24]</sup> bearing an N-terminal SpyTag.

Our first dimer was Outer surface protein C (OspC), an important vaccine candidate from *Borrelia burgdorferi*, the bacterium causing Lyme disease. OspC is expressed both during transmission from the tick and upon entry into the mammalian host.<sup>[25]</sup> We expressed an N-terminally truncated fragment of OspC solubly in *E. coli* with SpyTag003 at its N-terminus. The OspC  $\Delta$ 19 C129S fragment, a parallel dimer (C2 symmetry, Figure 3A), is highly immunogenic and

induces protective immunity against *B. burgdorferi* infection.<sup>[25]</sup>

Newcastle Disease Virus (NDV) is a paramyxovirus and a particular danger for poultry farming. NDV's hemagglutinin-neuraminidase (HN) is crucial in host-cell entry and egress and, like many paramyxovirus antigens, exists as a loosely-associated tetramer of two approximately antiparallel dimers.<sup>[26,27]</sup> We expressed an N-terminally truncated fragment of HN (termed NDV HN), aiming to generate a C2 dimer (Figure 3A) bearing SpyTag003 at its C-terminus. The two C-termini of the HN dimer in PDB ID: 3T1E are > 7 nm apart.<sup>[26]</sup>

Influenza virus is a persistent challenge for both human and veterinary health.<sup>[28]</sup> Annual human epidemics of influenza cause  $\approx$  3–5 million cases of severe illness, with 290 000–650 000 deaths.<sup>[28]</sup> Current influenza vaccines may fail to induce potent protection, especially in people over 65.<sup>[29]</sup> Furthermore, vaccines produced in eggs are slow to scale up and antigen egg-adaptation can lower effectiveness.<sup>[30]</sup> Current vaccines mostly induce antibodies to hemagglutinin (HA) but not neuraminidase (NA), even though antibodies to both contribute to protection.<sup>[31]</sup> As a trimer with C3 symmetry, HA is well suited for genetic fusion to the 3-fold axis of various protein nanoparticles.<sup>[6,7]</sup> However, NA is a tetramer with C4 symmetry, complicating genetic fusion to self-assembling protein VLPs. Therefore, we explored whether each of these symmetries could be decorated on our VLP platform. Since influenza shows substantial diversity,<sup>[28]</sup> we tested our approach on antigens from distinct strains. For HA, we tested H3 from A/Aichi/2/1968 (termed H3 Aichi) and A/Victoria/361/2011 (termed H3 Vic) influenza strains. For NA, we tested N2 from A/Victoria/361/2011 (termed N2) and N1 from A/England/195/2009 (termed N1). As tetramers with dihedral symmetry (D2), we coupled two proteins of divergent size; *Streptomyces avidinii* streptavidin (60 kDa) and the very large *E. coli*  $\beta$ -galactosidase (483 kDa) (Figure 3A).

Antigens were conjugated with SpyCatcher003-mi3 at different molar ratios for 16 h at 4 °C and any insoluble aggregates removed by centrifugation. The amount of covalent VLP-Antigen conjugate formed at each coupling ratio was quantified using SDS-PAGE and gel densitometry. Apart from  $\beta$ -galactosidase, all antigens were efficiently displayed on SpyCatcher003-mi3 (Figure 3B,C, Figure S4A,B). When incubated at equimolar concentration of Tag and Catcher, most reactions produced minimal residual non-conjugated antigen (Figure 3B,C). This lack of free antigen subunits indicates that at a low antigen concentration, antigen coupling predominantly takes place though all SpyTags on each antigen (Figure 1D). With all tested antigens, near-quantitative coupling of all VLP SpyCatchers was achievable (Figure 3B), suggesting that steric hindrance did not block SpyCatcher003 reactivity even when large multimeric antigens were displayed. However, our panel of antigens suggests that both the size of antigen and orientation of its subunits can have an effect on coupling efficiency. OspC efficiently reacted through both subunits and saturated SpyCatcher003 at low VLP:antigen ratios (Figure 3B,C). Similarly, the two variants of influenza HA had minimal free subunits left at 1:1 and 1:1.5 molar ratios, indicating that the HA variants were mainly



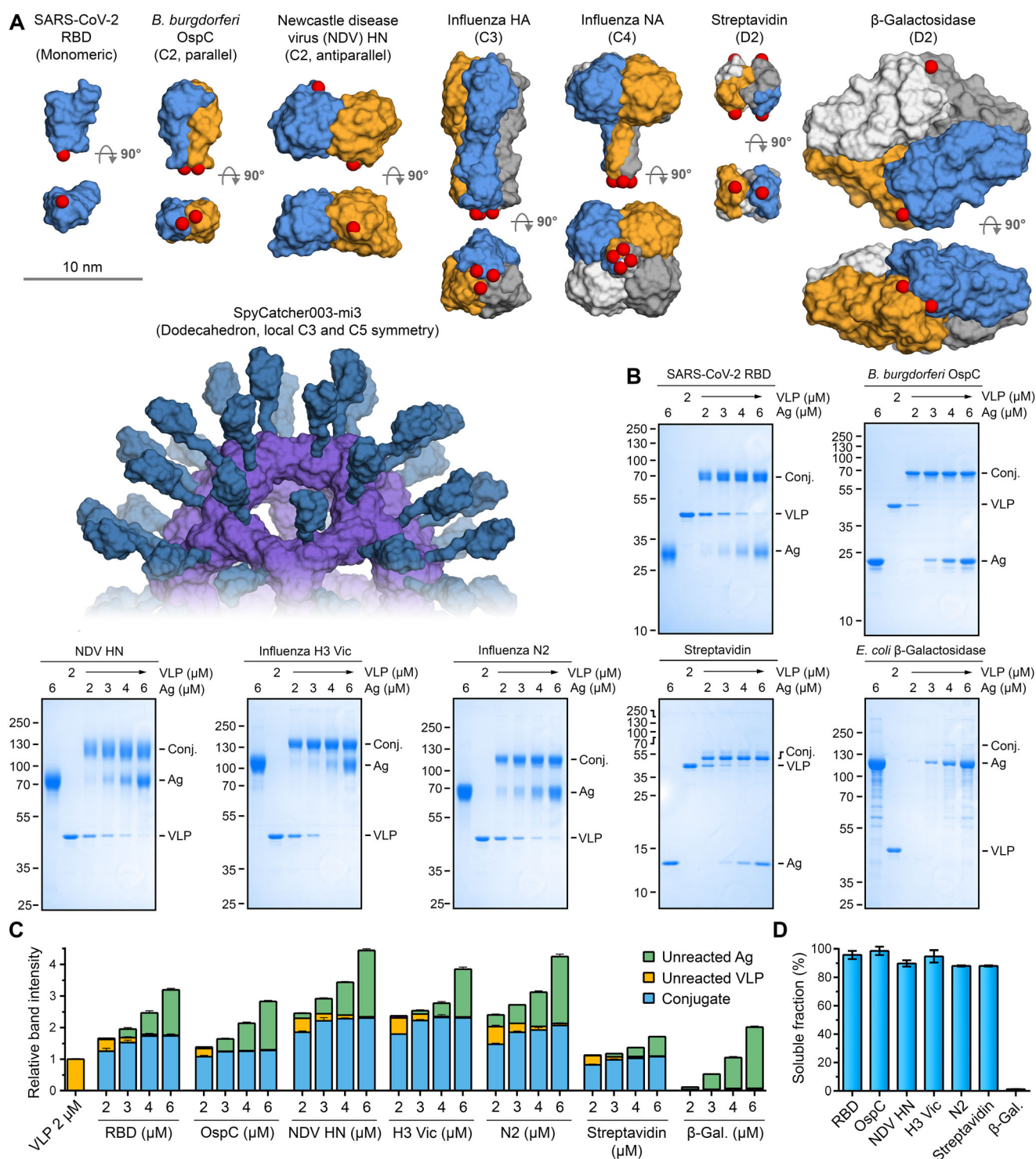


**Figure 3.** SpyCatcher003-mi3 particles allowed efficient display of antigens with different sizes and symmetries. A) Structures of the antigens with varying symmetry. Each antigen is shown in two orientations with space-filling model, with each chain in a different color. A model of SpyCatcher003-mi3 is presented at the same scale. PDB IDs: RBD: 6W41, OspC: 1G5Z, NDV HN: 3T1E, HA: 4UO0, NA: 2HTY (with tetramerization domain: 1USE), streptavidin: 1SWB,  $\beta$ -galactosidase: 6DRV. Red spheres indicate where the reactive peptide is fused. B) Coupling of model antigens at different molar VLP:antigen ratios. Samples were reacted for 16 h at 4°C, insoluble aggregates removed by centrifugation, and supernatant loaded on reducing SDS-PAGE before Coomassie staining. C) Quantification of VLP:antigen reactions. The intensity of each band from gel densitometry was divided by the intensity of the band of VLP alone at 2  $\mu$ M. Bars represent mean  $\pm$  s.d.,  $n = 3$ . D) Antigens with cyclic symmetry maintained good VLP solubility. Soluble fraction of antigens conjugated at 1:1 molar ratio was determined by densitometry (mean  $\pm$  s.d.,  $n = 3$ ). Some error bars are too small to be visible.

conjugated through all three SpyTags (Figure 3B,C, Figure S4A,B,C). In contrast, our NDV HN construct, an antiparallel dimer, required 3-fold antigen excess for VLP saturation, with more non-covalently coupled subunits present at the saturating level (i.e. coupled through only one tag of each dimer) (Figure 3B,C). For antigens with dihedral symmetry, streptavidin retained good VLP solubility but  $\beta$ -galactosidase led to almost complete loss of soluble VLP at all ratios (Figure 3B-D). This difference suggests that antigen size is critical when Tags are located on different faces of the antigen. We also established efficient co-display of HA and NA on VLPs; varying the ratio of antigens during conjugation allowed simple adjustment of display density (Figure S4D). This approach provides a simple way to create vaccine candidates mimicking the density of HA and NA on natural influenza virions.

Analysis of solubility does not necessarily reveal low levels of VLP crosslinking, structural changes in the VLP, or the presence of soluble aggregates. Therefore, we studied size distribution and monodispersity by dynamic light scattering (DLS). The hydrodynamic radius of non-conjugated SpyCatcher003-mi3 was 18.6 nm. The hydrodynamic radius of antigen-conjugated particles ranged from 19.5 nm (Streptavidin) to 28.3 nm (H3 Vic), consistent with antigen size (Figure 4A, Figure S5A–G). Both undecorated and antigen-decorated VLPs had narrow size distributions, indicating that antigen-decorated VLPs were monodisperse and VLP crosslinking was minimal. As expected, antigen-decorated particles exhibited distinct shapes and sizes depending on the displayed antigen, by transmission electron microscopy (TEM) after negative-staining (Figure 4B). H3 Vic trimers decorated on SpyCatcher003-mi3 pointed outwards in a radial arrangement, mimicking the orientation of HA on natural influenza virions. To investigate antigen stability after VLP decoration, we studied each dimeric antigen using ThermoFluor. OspC assembly on SpyCatcher003-mi3 resulted in a small increase of 0.9 °C in antigen  $T_m$  (Figure S6A). NDV HN decoration on SpyCatcher003-mi3 increased antigen  $T_m$  by 3.2 °C (Figure S6B). Therefore, Spy-VLP display maintains good antigen integrity and can even stabilize the structure of some multimeric antigens.

Having confirmed facile decoration of trimeric or tetrameric influenza antigens on our VLP platform, we investigated the magnitude and quality of immune responses. We validated efficient VLP coupling of H3 Vic, H3 Aichi or N1 by SDS-PAGE (Figure S7A). Mice were immunized intramuscularly with 0.1  $\mu$ g antigen doses using a homologous prime-boost regimen, along with AddaVax adjuvant (Figure 5A). Boosting was performed 2 weeks after prime, with blood sampling 4 weeks after the boost. We compared immunization with the same antigen dose of non-conjugated antigens or with influenza virion controls. For H3 Vic, wild-type Victoria/361/2011 virus (termed Vic/361) was the control. For H3 Aichi and N1, single-cycle influenza viruses (S-FLU) pseudotyped with matching HA or NA were controls. S-FLU is a promising viral vector vaccine: S-FLU virions infect host cells but lack a gene to express more HA, so are incapable of productive viral infection.<sup>[32]</sup> We analyzed antibody titers using a cell-based assay. Serum samples are incubated with

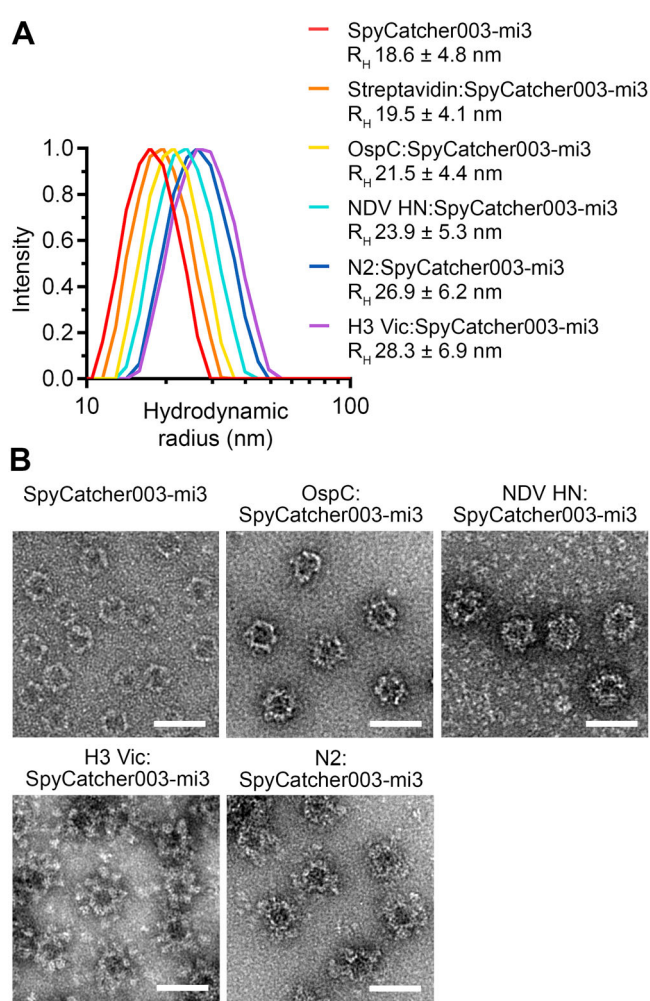


**Figure 4.** Particle size-distribution after VLP decoration of antigens of various symmetry. A) Hydrodynamic radius for SpyCatcher003-mi3 particles, with or without conjugation to antigens (mean  $\pm$  s.d.; for H3 Vic  $n = 2$  independent experiments; for all other samples  $n = 3$ ). B) TEM of negative-stained antigen-decorated SpyCatcher003-mi3 VLPs. Scale-bar: 50 nm.

cells expressing surface H3 or N1. Then cell-bound antibodies are detected using HRP-conjugated antibody. Both H3 Vic and N1, when conjugated to SpyCatcher003-mi3, induced higher median antibody titers than free antigen (7-fold for H3 Vic, 490-fold for N1, Figure 5B–D). VLP-display of H3 Aichi slightly increased the titer but this difference was not statistically significant (Figure 5C). H3 Vic displayed on the VLP induced 14-fold higher median titers than wild-type virus, while both H3 Aichi:VLP and N1:VLP induced titers similar to S-FLU (Figure 5B–D).

As an alternative method for analyzing titer, we used indirect ELISA with antigens coated on a microtiter plate. The results largely matched the cell-based assay, with both H3 Vic:VLP and N1:VLP giving significantly higher titers than free antigens (Figure S7B–D). In contrast to the cell-based assay, in indirect ELISA all tested viral vectors had titers significantly lower than what was induced by VLP-displayed antigens (Figure S7B–D).



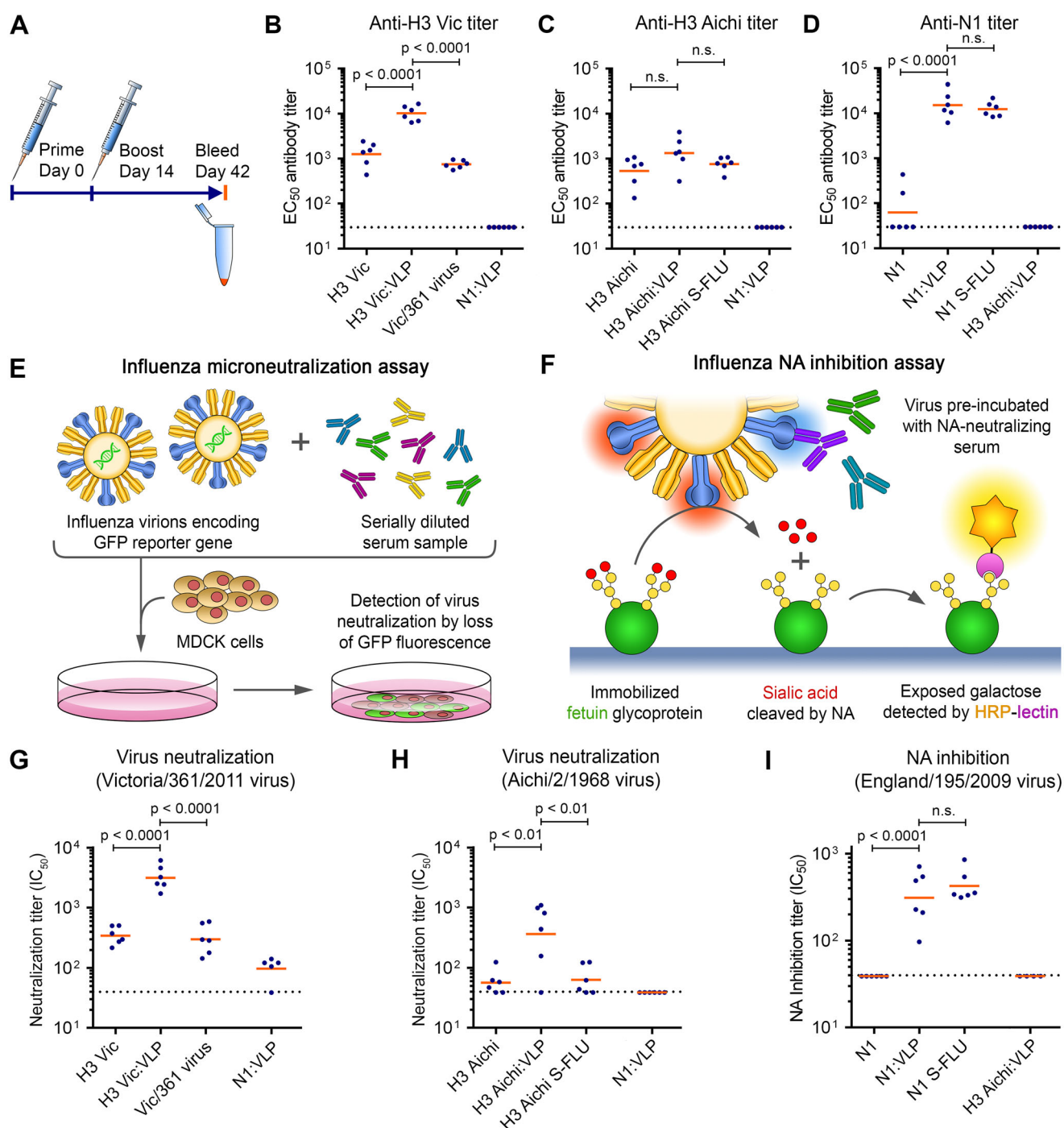


**Figure 5.** Display of trimeric or tetrameric influenza antigens on SpyCatcher003-mi3 enhanced antibody titre. A) Immunization schedule. B) Antibody titer against H3 Vic from mice primed and boosted with free H3 Vic, H3 Vic displayed on SpyCatcher003-mi3 (H3 Vic:VLP), or Vic/361 influenza virus. Each dot represents one mouse and the mean is indicated in orange.  $n=6$ . Sera were assayed against plasma membrane-bound H3 Vic. Serum from mice immunized with N1:VLP was a negative control. C) As for (B) with H3 Aichi. D) As for (B) with N1. Serum from immunizing with H3 Aichi:VLP was a negative control. E) Schematic of microneutralization assay. Neutralization potency is quantified through the decrease in GFP in cells incubated with virus pre-mixed with serum. F) Schematic of NA inhibition assay. Inhibition of NA catalytic activity is quantified through decrease of lectin-HRP binding to immobilized fetuin in the presence of NA-neutralizing antibodies. G) VLP-display enhanced virus-neutralizing activity from H3 Vic immunization. Microneutralization assay on serum following each immunization route, tested against A/Victoria/361/2011 influenza. Serum from immunizing with N1:VLP was a negative control.  $n=6$ , except N1:VLP  $n=5$ . H) Microneutralization assay as in (G) but for H3 Aichi and A/Aichi/2/1968 virus. I) NA inhibition assay for mice immunized with free N1, N1 displayed on VLP, or matching S-FLU. Serum from immunizing with H3 Aichi:VLP was a negative control.  $n=6$ , except H3 Aichi:VLP  $n=4$ . Dashed lines indicate limit of detection (1:40 dilution). Significance was analyzed using log<sub>10</sub>-transformed data and one-way ANOVA with Bonferroni correction. n.s. = not significant.

Beyond the amount of antibodies, it is important to evaluate antibody efficacy. We studied the functionality in a virus microneutralization assay for HA-specific antibodies (Figure 5E).<sup>[32]</sup> SpyCatcher003-mi3 display of H3 variants improved the median neutralization titers by 8.5–12 fold compared to free antigen or virus-based controls (Figure 5G,H). To confirm specificity of neutralizing antibodies, we assayed the sera against S-FLU pseudotyped with H3 Vic or H3 Aichi, giving similar results (Figure S7E,F).

The potency of NA-specific antibodies in inhibition of NA catalysis was studied using an enzyme-linked lectin assay (ELLA) (Figure 5F).<sup>[33]</sup> NA inhibition is an independent correlate of protection against influenza in clinical trials.<sup>[31]</sup> VLP-conjugated N1 showed potent NA inhibition, while none of the samples from immunization with free N1 showed detectable inhibition (Figure 5I). Similar to N1:VLP, A/England/195/09 S-FLU induced antibodies with potent inhibition of NA (Figure 5I).

To investigate if antigen VLP-display increased the functionality of the induced antibodies, we calculated  $IC_{50}/EC_{50}$  ratios. Only samples with above-threshold signal in both assays were included. VLP-display of H3 Vic slightly increased the mean  $IC_{50}/EC_{50}$  ratio compared to free antigen, but this difference was not statistically significant (Figure S7G). In contrast, VLP-display of H3 Aichi significantly increased  $IC_{50}/EC_{50}$ , indicating improved antibody functionality (Figure S7H). It was not possible to calculate  $IC_{50}/EC_{50}$  for free N1, because  $IC_{50}$  was below detection threshold. N1:VLP and the matching S-FLU gave similar  $IC_{50}/EC_{50}$ , indicating similar antibody functionality (Figure S7I). Taken together, the display of antigens on the SpyCatcher003-mi3 platform not only increased antibody titers but can also improve antibody functionality.

## Discussion

Nature is able to fabricate atomically precise megadalton assemblies, which usually depend on multiple weak interactions evolved over numerous generations.<sup>[3]</sup> Stable synthetic assemblies on this size-scale may benefit from modular covalent conjugations, so it is important to advance their scope in nanoassembly. We have shown that modular amidation through SpyCatcher003 enables nanoassembly of diverse cyclic protein symmetries on a dodecahedral 60-mer nanoparticle scaffold. Such generality is an important step towards the development of a broadly applicable platform to enhance the speed and efficiency of vaccine development.

Recombinant proteins, especially those from pathogens, often have marginal stability.<sup>[6–8]</sup> Therefore, linking many copies of such proteins on a single nanoparticle faces challenges from misfolding, aggregation or slow reaction near a crowded surface.<sup>[9]</sup> We observed that SpyCatcher003-mi3 allows display of antigens with diverse sizes and multimeric structures. Coupled particles were monodisperse by DLS, while VLP conjugation had a small thermostabilizing effect on coupled antigens. Despite the D2 symmetry of streptavidin and approximately antiparallel orientation of the NDV HN

protein dimer, both were successfully decorated on SpyCatcher003-mi3 while retaining high solubility. Similarly, all tested influenza antigens exhibited good solubility after VLP decoration. In contrast, particles decorated with the D2 symmetric  $\beta$ -galactosidase almost completely aggregated. These data suggest that with large antigens, dihedral symmetry of antigen subunits can lead to antigen-mediated VLP crosslinking and aggregation. Cyclic symmetry orients the binding sites in a single direction and is favored for membrane-anchored antigens.<sup>[34]</sup> C3 is likely to be the most common symmetry among oligomeric antigens.<sup>[6–8]</sup> We did not consider antigens with cubic symmetry (e.g. icosahedral shells) or unbounded symmetry (e.g. helical filaments),<sup>[34]</sup> since such proteins should already have sufficient multivalency to promote strong immune response.<sup>[8]</sup>

Owing to the improved properties of SpyCatcher003, the SpyCatcher003-mi3 platform exhibits high stability and activity. The platform can be expressed to high yields in *E. coli* and purified without affinity chromatography, through scalable and cost-efficient ammonium sulfate precipitation and SEC. mi3 is based on an enzyme from a hyperthermophilic marine bacterium.<sup>[14,15]</sup> Thus, existing human seroreactivity against the particle itself is unlikely. Here, we detected anti-SpyTag/SpyCatcher antibodies in almost all human serum samples, while anti-SpyTag003/SpyCatcher003 had 5-fold decreased response. This reduced response is understandable, considering the 18 amino acid substitutions in the 003 pair.<sup>[16]</sup> How pre-existing anti-platform antibodies shape vaccine response has been investigated in several studies: for Hepatitis B surface antigen (HBsAg), existing responses to the VLP or a homologous prime-boost regimen do not impair later antigen-specific immune response.<sup>[35,36]</sup> In contrast to VLPs, anti-platform responses are problematic where cell infection is required for vaccine function, for example, adenoviral vectors.<sup>[37]</sup> Pre-existing human antibodies against the orthogonal SnoopTag/SnoopCatcher pair were detected in only 25% of people. Therefore, SnoopTag-mediated assembly in heterologous prime-boost immunization is an option, if repeated use of SpyCatcher003-mi3 is ever problematic. Tag/Catcher conjugation has been applied for decoration of CAR-T cells and in vivo imaging,<sup>[10]</sup> where the consequences of pre-existing immune responses for clinical development are likely to be more important.

Immunization with influenza HA or NA displayed on Spy-VLPs gave superior antibody functionality compared to free antigen, which may be associated with both the multivalency and the orientation being similar to natural virions. Previous strategies to create HA-containing nanoassemblies include budding of influenza VLPs from cells, as well as genetic fusion of HA to protein cages.<sup>[38]</sup> While this work was in progress, the original SpyTag/SpyCatcher was used for multimerization of a truncated and non-glycosylated monomeric HA head.<sup>[39]</sup> Modular nanoassembly of HA by SpyCatcher003-mi3 allows VLP stockpiling, which may help timely response to new influenza pandemics and the yearly variation of circulating influenza strains.<sup>[28–30]</sup> Modular vaccine assembly and tunable antigen density may also help to ensure high immunogenicity and access to the broadly neutralizing epitopes in the HA stem domain.<sup>[6]</sup> In contrast



to HA, few studies have investigated display of NA on protein VLPs.<sup>[40, 41]</sup>

## Conclusion

Spy-VLP display may facilitate the next generation of recombinant influenza vaccines, inducing potent activity against both HA and NA. Together, we demonstrate that the SpyCatcher003-mi3 platform is well suited for the display of complex antigens of diverse symmetry. Beyond vaccines, Spy-based nanoassembly has enabled advances in catalysis, biomaterials and diagnostics, where applicability to different symmetry states may be similarly beneficial.<sup>[42, 43]</sup>

## Acknowledgements

R.R., A.C.A., J.R.B., S.J.D. and M.H. were funded by the Medical Research Council (MR/P001351/1). This UK funded award is part of the EDCTP2 programme supported by the European Union. S.J.D. is also a Lister Institute Research Prize Fellow, a Jenner Investigator and a Wellcome Trust Senior Fellow (106917/Z/15/Z). R.R. was supported by the Finnish Cultural Foundation and the Foundations' Post Doc Pool with grant 00191229. P.R. and A.R.T. were funded by the Chinese Academy of Medical Sciences (CAMS) Innovation Fund for Medical Sciences (CIFMS), China (grant number: 2018-I2M-2-002) and Townsend-Jeantet Prize Charitable Trust (Charity Number 1011770). T.K.T. was funded by the EPA Cephalosporin Early Career Teaching and Research Fellowship and Townsend-Jeantet Prize Charitable Trust (Charity Number 1011770). T.A.B. was funded by the Medical Research Council (MR/L009528/1 and MR/S007555/1), with the Wellcome Trust Centre for Human Genetics supported by Wellcome Centre grant 203141/Z/16/Z. At the University of Oxford we thank Angela Minassian for VAC063 clinical trial sample access, Niels Wicke for assistance with TEM, and David Staunton of the Department of Biochemistry Biophysical Suite for assistance with particle analysis.

## Conflict of interest

M.H. is an inventor on a patent regarding spontaneous amide bond formation (EP2534484) and a patent application regarding SpyTag003:SpyCatcher003 (UK Intellectual Property Office 1706430.4). M.H. and S.J.D. are SpyBiotech co-founders, shareholders and consultants. A.R.T. is an inventor on a patent relating to S-FLU (EP2758525A2).

**Keywords:** bioconjugation · nanoparticle · nanotechnology · SpyTag · vaccines

- [1] A. M. Smith, A. M. Mohs, S. Nie, *Nat. Nanotechnol.* **2009**, *4*, 56–63.
- [2] F. Wang, S. He, H. Wang, S. Zhang, C. Wu, H. Huang, Y. Pang, C. K. Tsung, T. Li, *Chem. Sci.* **2019**, *10*, 7755–7761.
- [3] J. T. Huiskonen, *Biosci. Rep.* **2018**, *38*, BSR20170203.

- [4] M. R. Green, G. M. Manikhas, S. Orlov, B. Afanasyev, A. M. Makhson, P. Bhar, M. J. Hawkins, *Ann. Oncol.* **2006**, *17*, 1263–1268.
- [5] M. Li, J. S. Chen, M. Cotlet, *ACS Photonics* **2019**, *6*, 1451–1457.
- [6] M. Kanekiyo, M. G. Joyce, R. A. Gillespie, J. R. Gallagher, S. F. Andrews, H. M. Yassine, A. K. Wheatley, B. E. Fisher, D. R. Ambrozak, A. Creanga, K. Leung, E. S. Yang, S. Boyoglu-Barnum, I. S. Georgiev, Y. Tsybovsky, M. S. Prabhakaran, H. Andersen, W.-P. Kong, U. Baxa, K. L. Zephir, J. E. Ledgerwood, R. A. Koup, P. D. Kwong, A. K. Harris, A. B. McDermott, J. R. Mascola, B. S. Graham, *Nat. Immunol.* **2019**, *20*, 362.
- [7] J. Marcandalli, B. Fiala, S. Ols, M. Perotti, W. de van der Schueren, J. Snijder, E. Hodge, M. Benhaim, R. Ravichandran, L. Carter, W. Sheffler, L. Brunner, M. Lawrenz, P. Dubois, A. Lanzavecchia, F. Sallusto, K. K. Lee, D. Velesler, C. E. Correnti, L. J. Stewart, D. Baker, K. Loré, L. Perez, N. P. King, *Cell* **2019**, *176*, 1420–1431.
- [8] A. Gomes, M. Mohsen, M. Bachmann, A. C. Gomes, M. Mohsen, M. F. Bachmann, *Vaccines* **2017**, *5*, 6.
- [9] K. D. Brune, M. Howarth, *Front. Immunol.* **2018**, *9*, 1432.
- [10] A. H. Keeble, M. Howarth, *Chem. Sci.* **2020**, *11*, 7281–7291.
- [11] K. D. Brune, D. B. Leneghan, I. J. Brian, A. S. Ishizuka, M. F. Bachmann, S. J. Draper, S. Biswas, M. Howarth, *Sci. Rep.* **2016**, *6*, 19234.
- [12] D. B. Leneghan, K. Miura, I. J. Taylor, Y. Li, J. Jin, K. D. Brune, M. F. Bachmann, M. Howarth, C. A. Long, S. Biswas, *Sci. Rep.* **2017**, *7*, 1–14.
- [13] A.-M. C. Andersson, C. M. Buldun, D. J. Pattinson, S. J. Draper, M. Howarth, *Sci. Rep.* **2019**, *9*, 4625.
- [14] Y. Hsia, J. B. Bale, S. Gonen, D. Shi, W. Sheffler, K. K. Fong, U. Nattermann, C. Xu, P.-S. Huang, R. Ravichandran, S. Yi, T. N. Davis, T. Gonen, N. P. King, D. Baker, *Nature* **2016**, *535*, 136–139.
- [15] T. U. J. Bruun, A.-M. C. Andersson, S. J. Draper, M. Howarth, *ACS Nano* **2018**, *12*, 8855–8866.
- [16] A. H. Keeble, P. Turkki, S. Stokes, I. N. A. Khairil Anuar, R. Rahikainen, V. P. Hytönen, M. Howarth, *Proc. Natl. Acad. Sci. USA* **2019**, *116*, 26523–26533.
- [17] M. Zhao, M. Vandersluis, J. Stout, U. Haupts, M. Sanders, R. Jacquemart, *Vaccine* **2019**, *37*, 5491–5503.
- [18] O. S. Kumru, S. B. Joshi, D. E. Smith, C. R. Middaugh, T. Prusik, D. B. Volkin, *Biologicals* **2014**, *42*, 237–259.
- [19] R. Mortensen, T. N. Nissen, S. Fredslund, I. Rosenkrands, J. P. Christensen, P. Andersen, J. Dietrich, *Sci. Rep.* **2016**, *6*, 22030.
- [20] S. Amelung, A. Nerlich, M. Rohde, B. Spellerberg, J. N. Cole, V. Nizet, G. S. Chhatwal, S. R. Talay, *Cell. Microbiol.* **2011**, *13*, 1200–1211.
- [21] K. D. Brune, C. M. Buldun, Y. Li, I. J. Taylor, F. Brod, S. Biswas, M. Howarth, *Bioconjugate Chem.* **2017**, *28*, 1544–1551.
- [22] J. N. Weiser, D. M. Ferreira, J. C. Paton, *Nat. Rev. Microbiol.* **2018**, *16*, 355–367.
- [23] Q. Zhang, J. Bernatoniene, L. Bagraade, A. J. Pollard, T. J. Mitchell, J. C. Paton, A. Finn, *Eur. J. Immunol.* **2006**, *36*, 46–57.
- [24] N. Lurie, M. Saville, R. Hatchett, J. Halton, *N. Engl. J. Med.* **2020**, *382*, 1969–1973.
- [25] D. G. Edmondson, S. Prabhakaran, S. J. Norris, A. J. Ullmann, J. Piesman, M. Dolan, C. Probst, C. Radzinski, W. Stöcker, L. Komorowski, *Clin. Vaccine Immunol.* **2017**, *24*, e00306-16.
- [26] P. Yuan, K. A. Swanson, G. P. Leser, R. G. Paterson, R. A. Lamb, T. S. Jardetzky, *Proc. Natl. Acad. Sci. USA* **2011**, *108*, 14920–14925.
- [27] T. A. Bowden, M. Crispin, D. J. Harvey, E. Y. Jones, D. I. Stuart, *J. Virol.* **2010**, *84*, 6208–6217.
- [28] A. D. Iuliano, K. M. Roguski, H. H. Chang, D. J. Muscatello, *Lancet* **2018**, *391*, 1285–1300.
- [29] H. Q. McLean, M. G. Thompson, M. E. Sundaram, B. A. Kieke, M. Gaglani, K. Murthy, P. A. Piedra, R. K. Zimmerman, M. P.



- Nowalk, J. M. Raviotta, M. L. Jackson, L. Jackson, S. E. Ohmit, J. G. Petrie, A. S. Monto, J. K. Meece, S. N. Thaker, J. R. Clippard, S. M. Spencer, A. M. Fry, E. A. Belongia, *J. Infect. Dis.* **2015**, *211*, 1529–1540.
- [30] J. A. Tree, C. Richardson, A. R. Fooks, J. C. Clegg, D. Looby, *Vaccine* **2001**, *19*, 3444–3450.
- [31] F. Krammer, R. A. M. Fouchier, M. C. Eichelberger, R. J. Webby, K. Shaw-Saliba, H. Wan, P. C. Wilson, R. W. Compans, I. Skountzou, A. S. Monto, *mBio* **2018**, *9*, e02332-17.
- [32] T. J. Powell, J. D. Silk, J. Sharps, E. Fodor, A. R. M. Townsend, *J. Virol.* **2012**, *86*, 13397–13406.
- [33] P. Rijal, B. B. Wang, T. K. Tan, L. Schimanski, P. Janesch, T. Dong, J. W. McCauley, R. S. Daniels, A. R. Townsend, K.-Y. A. Huang, *J. Virol.* **2020**, *94*, e01182-19.
- [34] D. S. Goodsell, A. J. Olson, *Annu. Rev. Biophys. Biomol. Struct.* **2000**, *29*, 105–153.
- [35] A. Marini, Y. Zhou, Y. Li, I. J. Taylor, D. B. Leneghan, J. Jin, M. Zaric, D. Mekhaieel, C. A. Long, K. Miura, S. Biswas, *Front. Immunol.* **2019**, *10*, 2931.
- [36] Clinical Trials Partnership, *Lancet* **2015**, *386*, 31–45.
- [37] A. K. Zaiss, H. B. Machado, H. R. Herschman, *J. Cell. Biochem.* **2009**, *108*, 778–790.
- [38] M. Kanekiyo, C. J. Wei, H. M. Yassine, P. M. McTamney, J. C. Boyington, J. R. R. Whittle, S. S. Rao, W. P. Kong, L. Wang, G. J. Nabel, *Nature* **2013**, *499*, 102–106.
- [39] J. Sharma, K. Shephardson, L. L. Johns, J. Wellham, J. Avera, B. Schwarz, A. Rynda-Apple, T. Douglas, *ACS Appl. Mater. Interfaces* **2020**, *12*, 18211–18224.
- [40] J. C. C. Lai, W. W. L. Chan, F. Kien, J. M. Nicholls, J. S. M. Peiris, J. M. Garcia, *J. Gen. Virol.* **2010**, *91*, 2322–2330.
- [41] F. S. Quan, M. C. Kim, B. J. Lee, J. M. Song, R. W. Compans, S. M. Kang, *Virology* **2012**, *430*, 127–135.
- [42] H. Kim, H. Choi, Y. Bae, S. Kang, *Biotechnol. Bioeng.* **2019**, *116*, 2843–2851.
- [43] A. Hagen, M. Sutter, N. Sloan, C. A. Kerfeld, *Nat. Commun.* **2018**, *9*, 2881.

Manuscript received: July 13, 2020

Accepted manuscript online: September 4, 2020

Version of record online: ■ ■ ■ ■ ■ ■ ■ ■ ■ ■

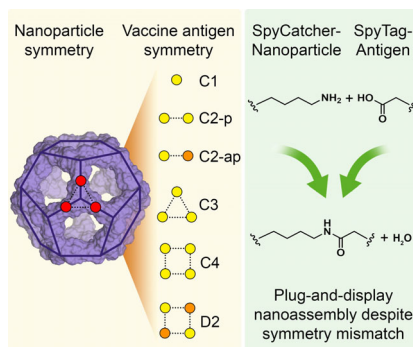
## Research Articles



## Vaccine Development

R. Rahikainen, P. Rijal, T. K. Tan, H.-J. Wu,  
A.-M. C. Andersson, J. R. Barrett,  
T. A. Bowden, S. J. Draper,  
A. R. Townsend,\*  
M. Howarth\* ————— ■■■■-■■■■

Overcoming Symmetry Mismatch in  
Vaccine Nanoassembly through  
Spontaneous Amidation



Nanoassembly can play a key role in generating effective vaccines for emerging (SARS-CoV-2) and established (influenza) pandemic threats. SpyTag-mediated display was used to adapt the nanocage to the challenge of bacterial or viral antigens with diverse cyclic and dihedral symmetries. Establishing display of both trimeric and tetrameric antigens may lead to an influenza vaccine with broader protection.

## Supporting Information

### **Overcoming Symmetry Mismatch in Vaccine Nanoassembly through Spontaneous Amidation**

*Rolle Rahikainen<sup>+</sup>, Pramila Rijal<sup>+</sup>, Tiong Kit Tan<sup>+</sup>, Hung-Jen Wu, Anne-Marie C. Andersson, Jordan R. Barrett, Thomas A. Bowden, Simon J. Draper, Alain R. Townsend,\* and Mark Howarth\**

anie\_202009663\_sm\_miscellaneous\_information.pdf

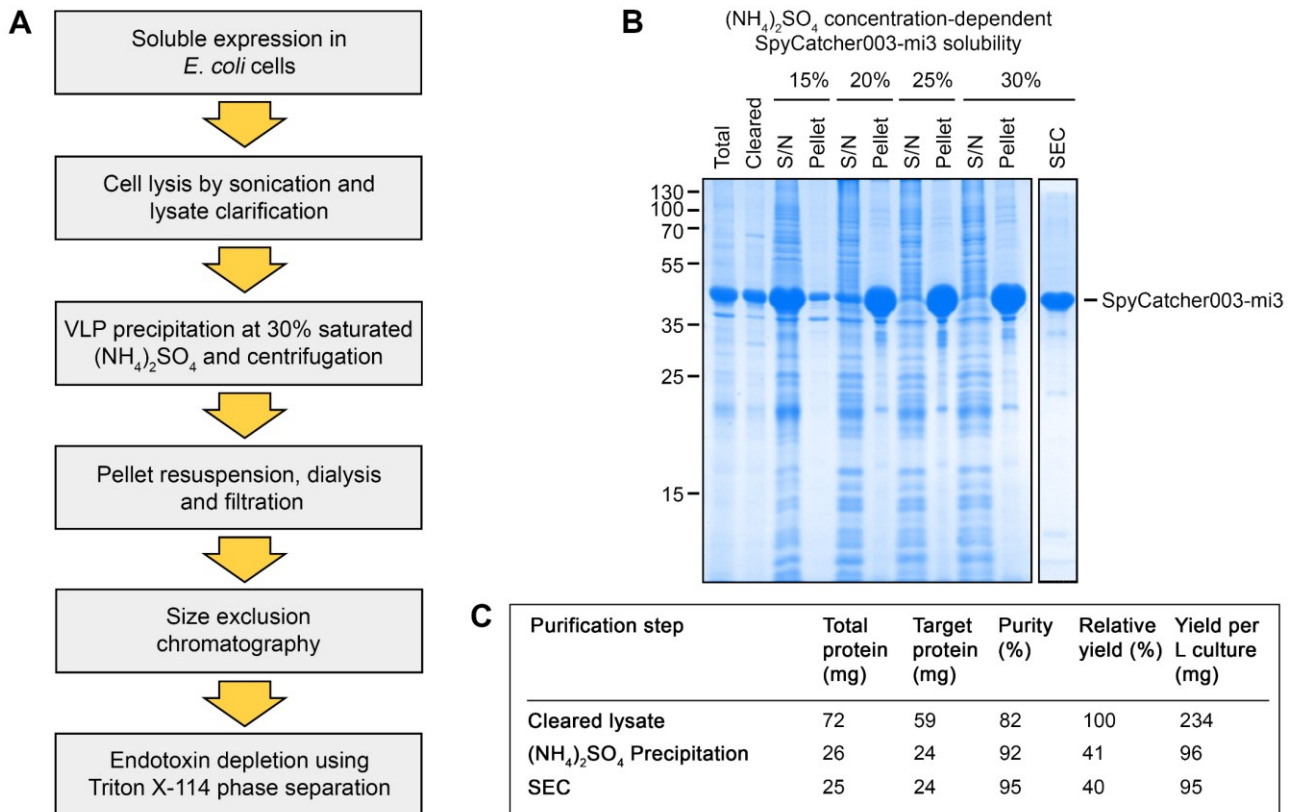


**Figure S1.** Affinity-independent Spy-VLP purification. (A) Process diagram for scalable SpyCatcher003-mi3 purification using (NH<sub>4</sub>)<sub>2</sub>SO<sub>4</sub> precipitation and size exclusion chromatography. (B) Nanoparticle purification using (NH<sub>4</sub>)<sub>2</sub>SO<sub>4</sub>. *E. coli* total lysate was centrifuged and filtered to give cleared lysate and incubated with increasing ammonium sulfate concentrations, as analyzed by SDS-PAGE with Coomassie staining. Supernatant (S/N) and pellet were compared and the 30% resuspended fraction was further purified by SEC. (C) Purification table, showing the yield and purity of a representative SpyCatcher003-mi3 purification using (NH<sub>4</sub>)<sub>2</sub>SO<sub>4</sub> and SEC.

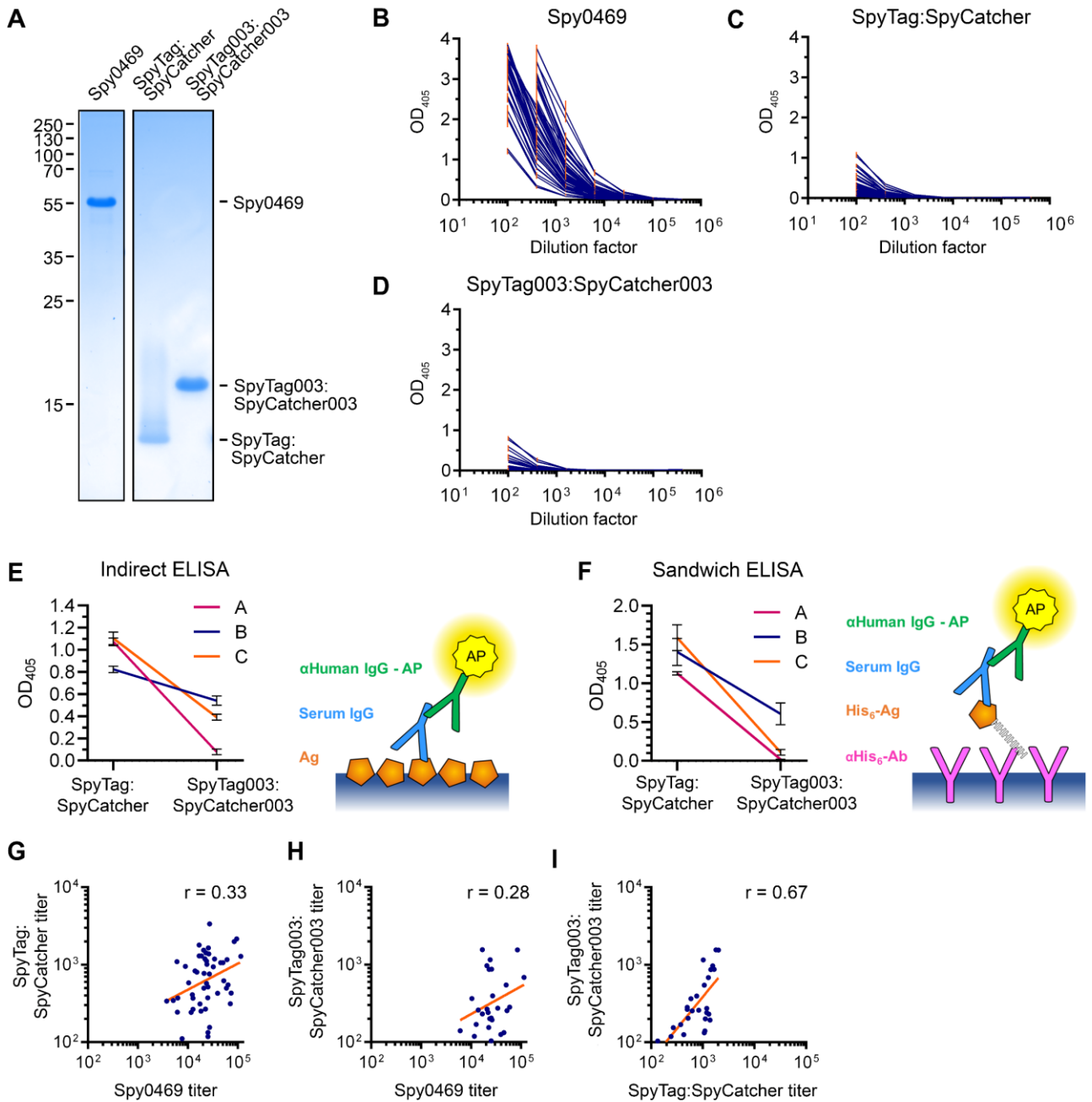


**Figure S2.** Testing of human sero-reactivity to SpyTag/SpyCatcher. (A) Antigen validation. Samples of antigens for pre-immunity analysis were resolved on non-reducing SDS-PAGE with Coomassie staining. As previously, after reaction with a short peptide, SpyCatcher showed gel-matrix interactions and migrated anomalously.<sup>[46]</sup> (B-D) Titration curves for antibody responses to each antigen. Each curve represents mean of two replicates for one person with error bars  $\pm 1$  s.d. presented as orange lines. In (B), data-points reaching detector saturation were omitted. (E-F) Comparison of indirect ELISA and sandwich ELISA for testing pre-existing antibodies to SpyTag/SpyCatcher or SpyTag003/SpyCatcher003 from three selected serum samples. Mean  $\pm 1$  s.d.,  $n = 2$ . Schematics of each assay are shown alongside. (G-I) Correlation analysis for pre-existing antibody titers against Tag/Catcher pairs and *S. pyogenes* control protein Spy0469. Samples with responses below the detection threshold for either protein were omitted. A blue dot represents one person, with the best-fit linear regression line in orange. Pearson correlation coefficient for  $\log_{10}$ -transformed data is shown; for (G)  $n = 51$ , for (H-I)  $n = 27$ .

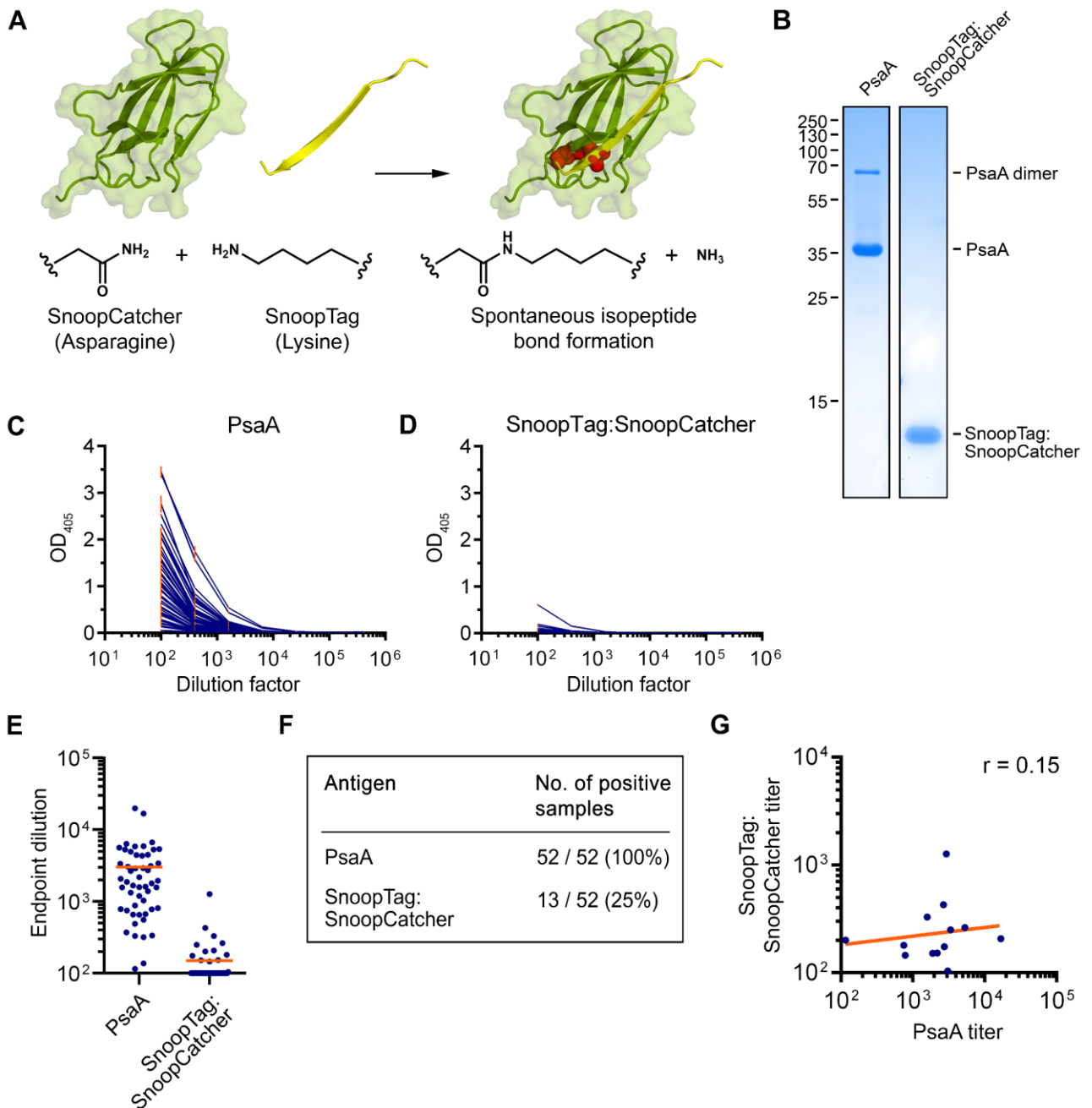


**Figure S3.** Testing of human sero-reactivity to SnoopTag/SnoopCatcher. (A) Schematic for bio-orthogonal SnoopTag/SnoopCatcher pair. An asparagine on SnoopCatcher (green) spontaneously forms an amide bond with a lysine on SnoopTag (yellow), based on PDB ID: 2WW8. Atoms forming the isopeptide bond are colored as red spheres. (B) Antigen validation. Samples of antigens for pre-immunity analysis were resolved on non-reducing SDS-PAGE with Coomassie staining. A fraction of PsaA ran as a disulfide-linked dimer. (C-D) Titration curves for antibody responses to each antigen. Each curve represents mean of two replicates for one person with error bars  $\pm 1$  s.d. presented as orange lines. (E) Pre-existing response to *S. pneumoniae* antigens. Antibody titer of serum from 52 healthy UK adults against the positive control PsaA or SnoopTag/SnoopCatcher. Each person is shown as a dot, with the mean in orange. (F) Summary of immune responses in (E). (G) Correlation analysis for pre-existing antibody titers against SnoopTag/SnoopCatcher and *S. pneumoniae* control protein PsaA. Samples with responses below the detection threshold for either protein were omitted. A blue dot represents one person, with the best-fit linear regression line in orange. Pearson correlation coefficient for  $\log_{10}$ -transformed data is shown.  $n = 13$ .

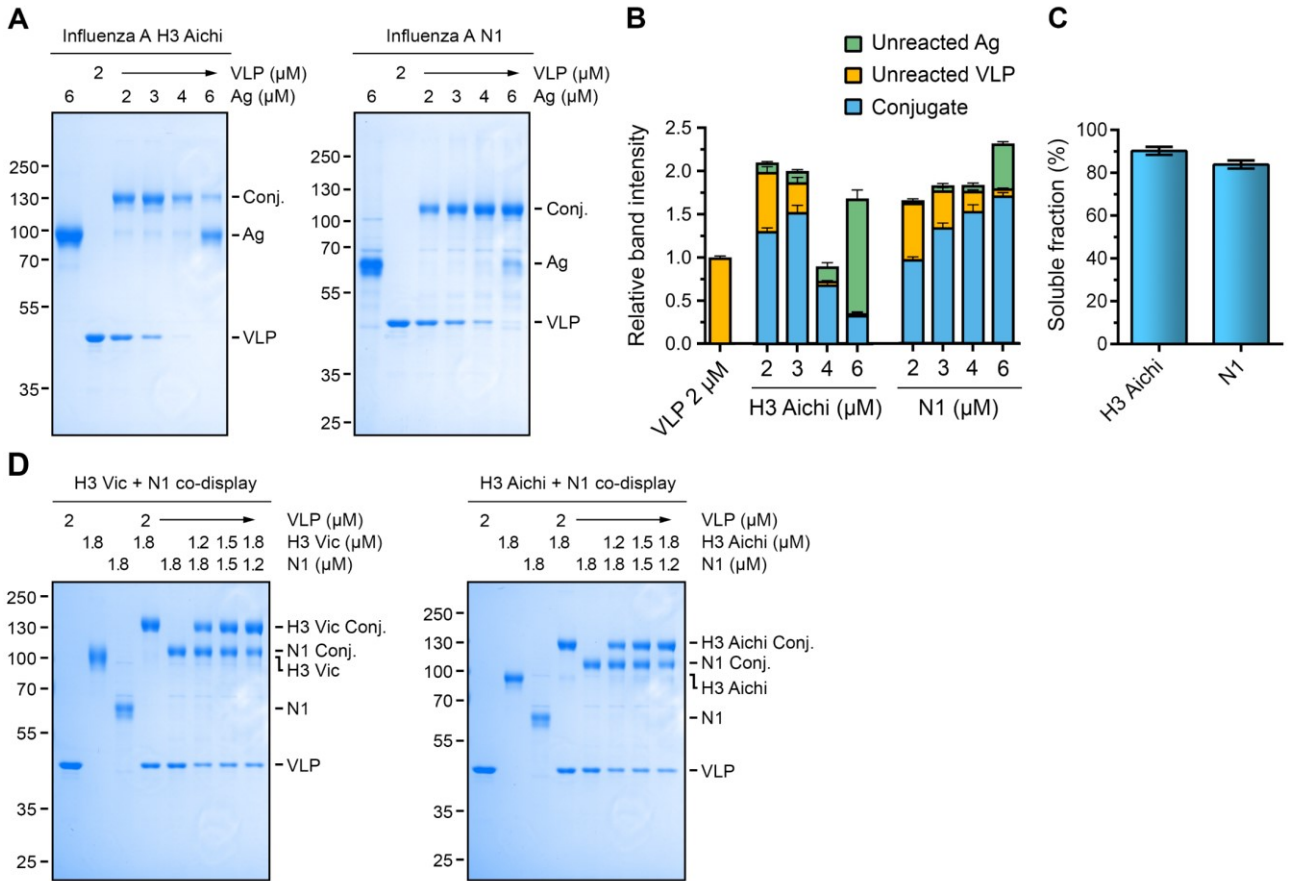


**Figure S4. VLP coupling to Influenza antigens.** (A) Coupling of H3 Aichi and N1 with SpyCatcher003-mi3 at different molar ratios. All samples were incubated for 16 h at 4 °C, insoluble aggregates removed by centrifugation, and supernatant loaded on reducing SDS-PAGE before Coomassie staining. Each gel is representative of three replicates. High excess of H3 Aichi led to decreased solubility of decorated VLPs. (B) Quantification of VLP:antigen reactions. The intensity of each band from gel densitometry was divided by the intensity of the band of VLP alone at 2 μM. Bars represent mean + 1 s.d., n = 3. (C) Soluble fraction of antigens conjugated at 1:1 molar ratio. Bars indicate mean ± 1 s.d., n = 3. (D) Co-display of H3 Victoria or H3 Aichi with N1 on a single particle. Antigens were mixed with the VLP at the indicated molar concentrations and incubated for 16 h at 4 °C, insoluble aggregates removed by centrifugation, and supernatant loaded on reducing SDS-PAGE before Coomassie staining.

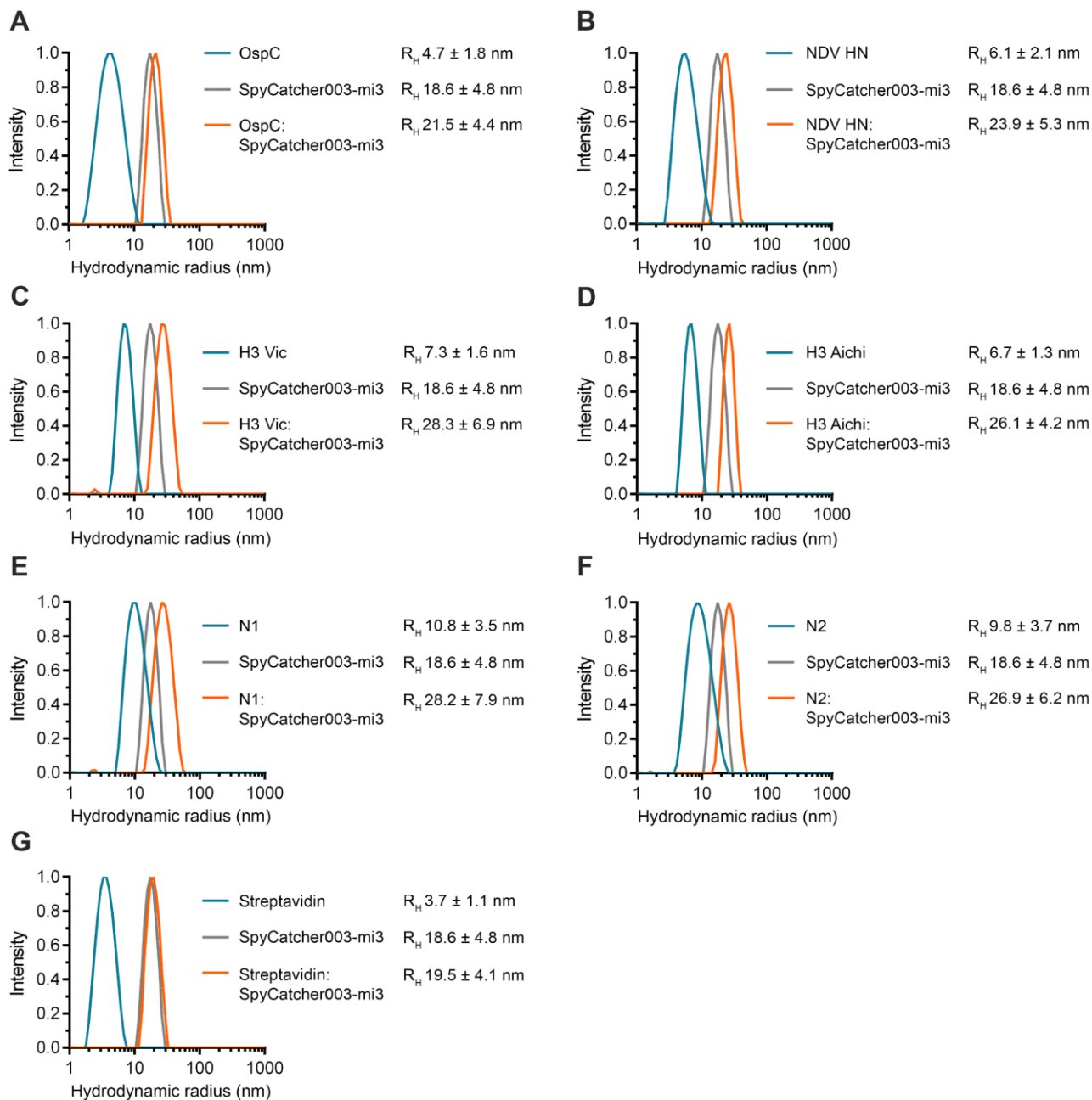


**Figure S5. Hydrodynamic size of antigens before and after VLP coupling.** (A-G) DLS for each multimeric antigen either alone or after conjugation with SpyCatcher003-mi3 at 1:1 molar ratio. For each antigen, mean hydrodynamic radius ( $R_H$ ) and s.d. of the particle size distribution of a representative experiment are presented.  $n = 2-3$  independent experiments for each sample.

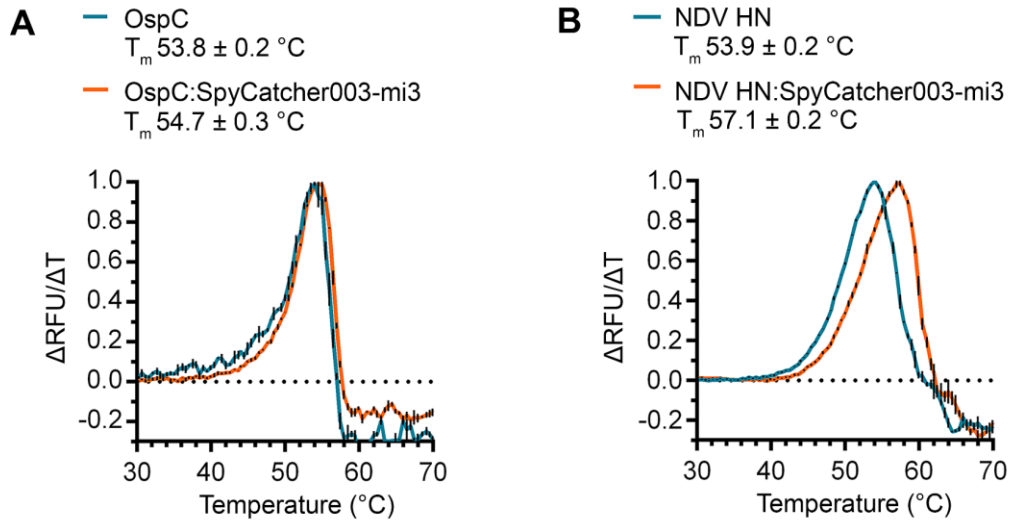


**Figure S6. Thermofluor assay of antigens after VLP coupling.** (A-B) Thermofluor assay for dimeric OspC and NDV HN antigens as free proteins or after VLP decoration. Graphs present the 1<sup>st</sup> derivative fluorescence signal ( $\Delta\text{RFU}/\Delta T$ ) of three replicates.  $T_m$  values are mean  $\pm$  1 s.d.,  $n = 3$ . Error bars, shown in black on the curves, are mean  $\pm$  1 s.d.,  $n = 3$ .

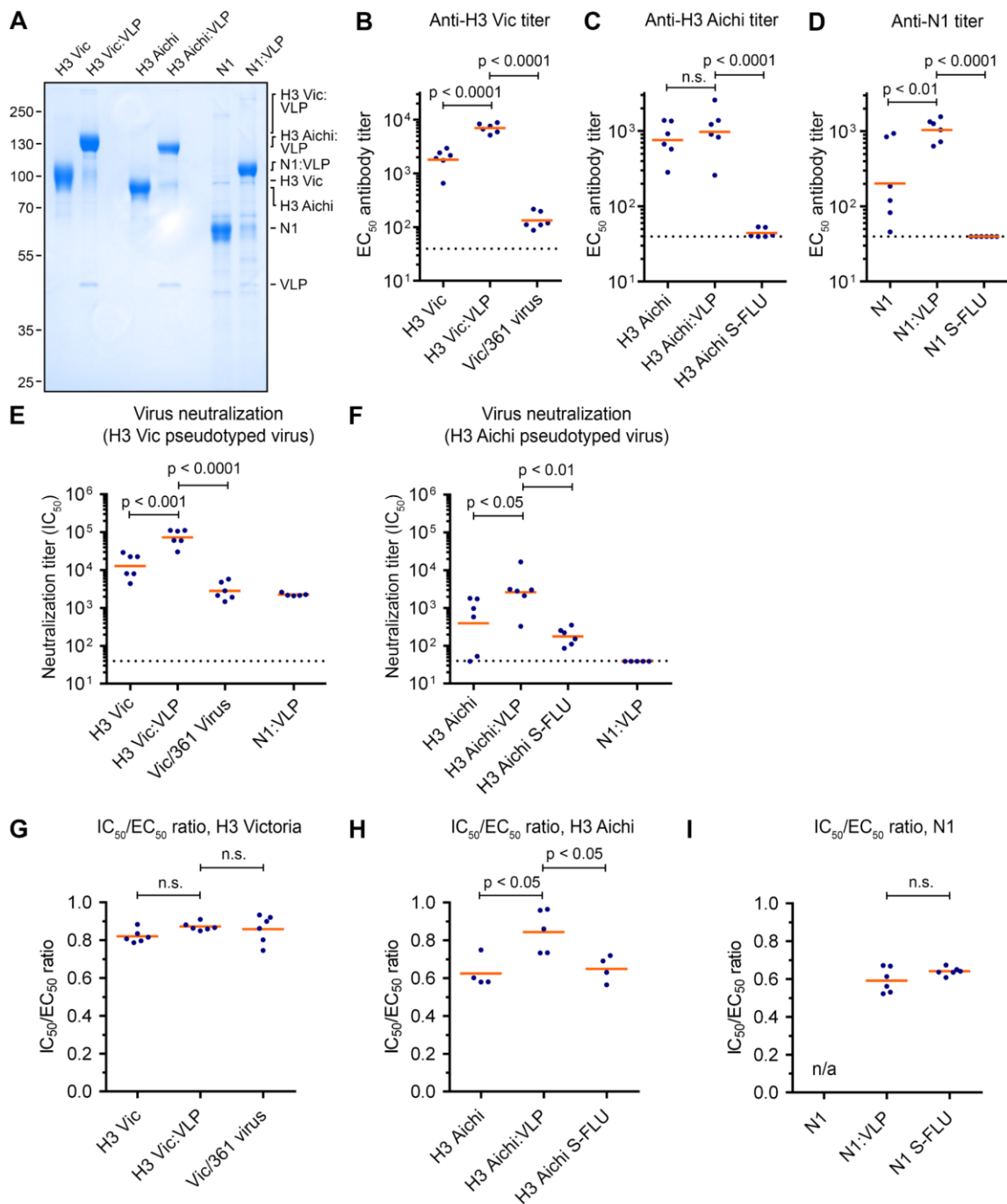


**Figure S7. Immunization with oligomeric Influenza antigens.** (A) Immunogens were resolved on SDS-PAGE with Coomassie staining to confirm successful coupling for 2  $\mu$ M VLP with 3  $\mu$ M H3 Vic, 3  $\mu$ M H3 Aichi or 4  $\mu$ M N1. (B-D) Indirect ELISA EC<sub>50</sub> titers for antibodies from H3 Vic, H3 Aichi and N1 immunizations. Each dot represents one mouse and the mean titer is indicated with an orange line. (E) Microneutralization assay to test antibody blockade of S-FLU infection of MDCK cells. Neutralization titer for the indicated S-FLU was determined for serum from mice immunized with H3 Vic, H3 Vic coupled to SpyCatcher003-mi3, or the matching S-FLU. Serum from mice immunized with N1:VLP was used as a negative control.  $n = 6$  for all groups except N1:VLP, where  $n = 5$ . Dashed lines indicate the lowest dilution factor (1:40) used in all assays. (F) As for (E) but with H3 Aichi. (G) IC<sub>50</sub>/EC<sub>50</sub> ratios for sera from H3 Vic immunizations. IC<sub>50</sub>/EC<sub>50</sub> ratios were calculated using log<sub>10</sub>-transformed IC<sub>50</sub> (microneutralization assay) and EC<sub>50</sub> (cell-based assay) titers.  $n = 6$  in each group. (H) As for (G) but with H3 Aichi.  $n = 4-5$  for each group. (I) As for (G) but with N1 EC<sub>50</sub> from ELLA. Below-threshold EC<sub>50</sub> titers prevent IC<sub>50</sub>/EC<sub>50</sub> calculation for free recombinant N1.  $n = 6$  in each group. In (B-I), statistical testing of log<sub>10</sub>-transformed EC<sub>50</sub> and IC<sub>50</sub> titers and IC<sub>50</sub>/EC<sub>50</sub> ratios was done using one-way ANOVA with Bonferroni correction.

**Table S1.** Amino acid sequence of proteins expressed. SpyTag and SpyTag003 are indicated in bold. His<sub>6</sub> tag (HHHHHH) and C-Tag (EPEA) are indicated with gray shading. The stop codon is indicated with a hyphen. SpyCatcher, SpyCatcher003, SnoopCatcher, Spy0469 and PsaA were cleaved with TEV protease to remove the His<sub>6</sub>-tag after purification. SUMO-SnoopTagJr was cleaved with SUMO protease Ulp1 to generate tagless SnoopTagJr. TEV protease and SUMO protease cleavage sites are indicated with a slash. SpyTag-RBD, NDV HN-SpyTag, H3 Vic-SpyTag003, H3 Aichi-SpyTag003, SpyTag-N1 and SpyTag-N2 are presented with N-terminal signal peptides. Proteins expressed in *E. coli* are shown with an N-terminal methionine. Table continued on the next page.

**SpyCatcher-mi3**

MGSSDSATHIKFSKRDEDGKELAGATMELRDSSGKTISTWISDGQVKDFLYLPGKYTFVETAAPDGYEVATAITFTVNEQQQVTVNGKATKGDAAHI  
GGSGGSGGSGGSMKMEELFKKKHIVAVLRANSVEEAKKALAVFLGGVHLIEITFTVPDADTVIKELSFLKEMGAIIGAGTVTSVEQARKAVESGAEFI  
VSPHLDEEISQFAKEKGVFYMFGVMTPTTELVKAMKLGHTILKLPGEVVGPFVKAMKGPFPNVKFPVPTGGVNLNDNVCEWFKAGVLAVGVGSAL  
VKGTPVEVAEKAKAFVEKIRGCTEGSGEPEA-

**SpyCatcher003-mi3**

MGSSVTTLSGLSGEQGPSGDMTTEEDSATHIKFSKRDEGRELAGATMELRDSSGKTISTWISDGHVKDFLYLPGKYTFVETAAPDGYEVATPIEFV  
NEDGQVTVDGEATEGDAHTGGSGGSGGSGSMKMEELFKKKHIVAVLRANSVEEAKKALAVFLGGVHLIEITFTVPDADTVIKELSFLKEMGAIIG  
AGTVTSVEQARKAVESGAEFIVSPHLDEEISQFAKEKGVFYMFGVMTPTTELVKAMKLGHTILKLPGEVVGPFVKAMKGPFPNVKFPVPTGGVNLND  
NVCEWFKAGVLAVGVGSALVKGTPVEVAEKAKAFVEKIRGCTEGSGEPEA-

**SpyCatcher**

MSYYHHHHHHHDYDIPTTENLYFQ/GAMVDTLSGLSSEQGSMDTIEEDSATHIKFSKRDEGKELAGATMELRDSSGKTISTWISDGQVKDFLYL  
PGKYTFVETAAPDGYEVATAITFTVNEQQQVTVNGKATKGDAAHI-

**SpyCatcher003**

MSYYHHHHHHHDYDIPTTENLYFQ/GAMVTTLSGLSGEQGPSGDMTTEEDSATHIKFSKRDEGRELAGATMELRDSSGKTISTWISDGHVKDFLYL  
PGKYTFVETAAPDGYEVATPIEFVNEEDGQVTVDGEATEGDAHTGSSGS-

**SnoopCatcher**

MGHHHHHHHGSGENLYFQ/GSGKPLRGAVFSLQKQHPDYDPIYGAIDQNGTYQNVRTGEDGKLTFKNLSGKYRLFENSEPAGYKPVQNKPIVAFQ  
IVNGEVRDVTSIVPQDIPATYEFTNGKHYYITNEPIPPK-

**SUMO-SnoopTagJr**

MGSWSHHHHHHHGSDEVNQAEKPEVKPEVKPETHINLKVSDGSSEIFFKIKKTTPLRLMEAFARQKQKEMDSLRFYLDGIRIQADQTPEDLDMED  
NDIIEAHREQIGG/GKLGSIKFKV/NKGS-

**Spy0469**

MGHHHHHHHGSGENLYFQ/GSGQAQEWTPRSVTEIKSELVLVDNVFTYTVKYGDTLSTIAEAMGIDVHVLGDINHIANIDLIFPDILTANYNQHGQ  
ATNLTVQAPASSPASVSHVPSSEPLQASATSQPTVPMAPPATPSDVPPTPFASAKPDSSVTASSETLSTNDVSTELSSSQKQPEVPQEAVPTPKA  
AETTEVEPKTDISEAPTSANRPVPNESASEEVSSAAPAQAPAEKEETSAPAAQKAVADTTSVATSNGLSYAPNHAYNPMNAGLQPQTAAAFKEEVAS  
AFGITSFSGYRPGDPGDHKGKLAIDFMVPENSALGDQVAQYAIHMAERGISYVIWQRFRYAPFASIYGPAITWNPMPDRGSITENHYDHVHVVSF  
NA-

**PsaA**

MGHHHHHHHGSGENLYFQ/GSGGSACASGKDDTSGQKLVVATNSIADITKNIAGDKIDLHSIVPIGQDPHEYELPEDVKKTSEADLIFYNGINLET  
GGNAWFTKLVENAKKTENKDYFAVSDGVDVIYLEGQNEKGDPAHWLNLENGIIFAKNIQKLSAKDPNNKEFYENLKEYTDKLDKLDKESKDKF  
NKIPAEKLLIVTSEGAFKYFSKAYGVPSAYIWEINTEEGTPEQIKTLVEKLRQTKVPSLFEVSSVDDRPMKTVSQDTNIPIYAIQIFDTSIAEQKKEGDSY  
YSMMKYNLDKIAEGLAK-

**SpyTag-RBD**

MNTQILVFALIAIPTNADKIGSGAHIVMVDAYKPTKSGSGSGSGSGTGNITNLCPFGEVFNATRFASVYAWNRRKRISNCVADSVLYNSASFSTFKCY  
GVSPKTLNDLCTFNVYADSFVIRGDEVQRQIAPGQTKIADYNYKLPDDFTGCVIAWNSNLDKSVGGNYNYLRLFRKSNLKPFRDISTEIYQAGST  
PCNGVEGFNCYFPLQSYGFQPTNGVGYQPYRIVVLSFELLHAPATVCGPKK-

**SpyTag003-OspC**

MGSSHHHHHHHSSGLVPRGSRGVPHIVMVDAYKRYKSGSGESGNSGKDGNASANSADSVKGPNLTEISKKITESNAVVLAVKEVETLLASIDELAT  
KAIGKIGNNGLEANQSKNTSLLSGAYAISDLIAEKLNLVKNELKEKIDTAKQSSTFTNKLKSEHAVLGLDNLDDNAQRILKHKHANKDKGAAEELK  
LFKAENLSKAAQDTLKNNAVKELTSPIVAESPCKP-

## Table S1 (continued)

### NDV HN-SpyTag

MGILPSPGMPALLSLVLSVLLMGCVAETGSMGASTPSDLVGIPTISRRAEEKITSALGSNQDQVVDRIYKQVALESPLALLNTETTMINAITSLSYQIN  
GAANNSGWGAPIHDPDFIGGIGKELIVDNASDVTSFYPSAFQEHLNFIAPPTTSGGCTRIPSFDMASATHYCYTHNVILSGCRDHSQYALGLVLR  
TATGRIFSTLRISLDDTQNRKSCVSATPLGCDMLCSKVTETEEDYNSAVPTLMAHGRLGFDGQYHEKLDVTTLFEDWVANYPGVGGGSFIDG  
RVWFVSYGGLKPNPSDSTVQEGKYVIYKRYNDTCPDEQDYQIRMAKSSYKPRFRGGKRIQQAISIKVSTSLGEDPVLTVPPNTVTLMGAEGRILTVG  
TSHFLYQRGSSYFSPALLYPMTVSNKATLHSPYTFNAFTRPGSIPQASARCPNSCVTVGVYDTPYPLIFYRNHTLRGVFGTMDLSEQARLNPAVA  
DSTSRSRITRVSSSSTKAAYTTSTCFKVVKTNKTYCLSAIEISNTLFGFEFRIVPLLVEILKNDGVREARSGGSGSGSGGSAHIVMVDAYKPTKSGSGTKH  
HHHHH-

### H3 Vic-SpyTag003

MKTIIALSYIFCLALGQDLPGNDSTATLCLGHHAVPNGTIVKITINDQIEVTNATELVQNSSIGEICDSPHQILDGENCTLIDALLGDPQCDGFQNK  
WDLFVERSKAYSNCYPYDVPDYASLRSLVASSGTLEFNNEFSNWTGVTQNGTSSACIRRSNNSFFSRLNLWTLHNFYKYPALNVTMPNNEQFDKLY  
WGVVHPGTDKDQIFLYAQSSGRITVSTKRSQQAVIPNIGSRPRIRNIPRSIYWTIVKPGDILLINSTGNLIAPRGYFKIRSGKSSIMRSDAPIKCNSEC  
ITPNGSIPNDKPFQNVNRITYGACPRYVKQSTLKLATGMRNVPEKQTRGIFGAIAGFIENGWEGMVDGWYGFRRHQNSEGRGQAADLKSTQAAID  
QINGKLNRLIGKTNEKFHQIEKEFSEVEGRIQDLEKYVEDTKIDLWSYNAELLVALENQHTIDLTDSEMKNLFEKTRRQLRENAEDMGNCGCFKIYHK  
DNACIGSIRNGTYDHDVYRDEALNRFQIKGVGSGSGSPSGYIPEAPRDGQAYVRKDGWVLLSTFLGGSGSGSGSGRGPVPHIVMVDAYKRYK  
GSHHHHHH-

### H3 Aichi-SpyTag003

MKTIIALSYIFCLALGQDLPGNDSTATLCLGHHAVPNGTLVKITITDDQIEVTNATELVQSSSTGKICNPNHRILDGIDCTLIDALLGDPHCDVFNQ  
WDLFVERSKAFSNCYPYDVPDYASLRSLVASSGTLEFITEGFTWTGVTQNGGNSACKRGPVSGGFFSRLNLWTKSGSTYVNLNVTMPNNDNFDKLY  
WGIHHPSTNQEQTSLYVQASGRVTVSTRSQQTIIPIGSRPWWVRLSSRSIYWTIVKPGDVLVINSNGNLIAAPRGYFKMRTGKSSIMRSDAPICTCI  
SECITPNGSIPNDKPFQNVNKITYGACPKYVQNTLKLATGMRNVPEKQTRGLFGAIAGFIENGWEGMIDGWYGFRRHQNSEGTQAAADLKSTQAA  
IDQINGKLNRLVIEKNEKFHQIEKEFSEVEGRIQDLEKYVEDTKIDLWSYNAELLVALENQHTIDLTDSEMKNLFEKTRRQLRENAEDMGNCGCFKIYHK  
CDNACIESIRNGTYDHDVYRDEALNRFQIKGVGSGSGSPSGYIPEAPRDGQAYVRKDGWVLLSTFLGGSGSGSGSGRGPVPHIVMVDAYKRYK  
GSHHHHHH-

### SpyTag-N1

MKANLLVLLCALAAADAADPHHHHHHSSSGSGAHIVMVDAYKPTKSGSGSGSGSDYDLQRVKQELLEEVKKEELQKVKEEIEAFVQELRKRGLV  
PRGSPSRISNTNFAAGQSVSVKLAGNSSLCPVSGWAIYSKDNSVRIGSKGDVVFIREPFISCSPLECRTFFLTQGALLNDKHSNGTIKDRSPYRTLMS  
CPIGEVPSPYNSRFESVAWSASACHDGINWLTIGISGPDNGAVAVLYKNGIITDTIKSWRNILRTQESEACVNGSCFTVMTDGPNSGQASYKIFRI  
EKGKIVKSVEMNAPNYHYEECSYDSEITCVCARDNWHGNSRNPVWVFNQNLQYQIGYICSGIFGDNPRPNDKTGSCGPVSSNGANGVKGFSEFKY  
NGVWIGRTKSISRNGFEMIWDPNGWTGTDNFNSIKQDIVGINEWSGYSGSFVQHPELTGLDCIRPCFWVVELIRGRPKENTIWTSGSSISFCGVNSD  
TVGWSWPDGAELPFTIDK-

### SpyTag-N2

MKANLLVLLCALAAADAADPHHHHHHSSSGSGAHIVMVDAYKPTKSGSGSGSGSDYDLQRVKQELLEEVKKEELQKVKEEIEAFVQELRKRGLV  
PRGSPSRSLNTTIEKICPKPAEYRNWVSKPQCIGTGFAPFSKDNSIRLSAGGDIWVTREPVSCDPDKCYQFALGQGTLLNNVHSNNTVRDRTPYRT  
LLMNELGVPFHLGTQVCIAWSSSCHDGKAWLHVCIITGDDKNATASFIYNGRLVDSVVSWSKEILRTQESECVINGTCTVVMTDGASGKADTK  
ILFIKEGKIVHTSTLSGSAQHVEECSCYPRYPGRVCRDNWKGNSRNPVIDINIKDHSIVSSYVCSGLVGDTPRKTDSSSSHCLDPNNEEGGHGVKG  
WAFDDGNDVWVMGRTINETSRLGYETFKVIEGWSNPKSKLQINRQVIVDRGDRSGYSGIFSVGKSCINRCFYVELIRGRKEETEVLWTSNSIVVFCG  
TSGTYGTGSWPDGADLNLMPI-

### Dead streptavidin-SpyTag

MAEAGITGTWYAQLGDTFIVTAGADGALTGTYEAAVGNAESRYVLTGRYDSAPATDGSGLTALGWTVAWKNNYRNAHSATTWSGQYVGGAEAR  
INTQWLLTSGTTEANAWKSTLVGHDTFTVKVPSAASGSGSGGSAHIVMVDAYKPT-

### SpyTag003- $\beta$ -galactosidase

MGSSHHHHHSSGLVPRGSRGPVPHIVMVDAYKRYKSGSGESGMTMITDSLAVVLQRRDWDENPGVTQLNRLAAHPPFASWRNSEEARTDRPSQ  
QLRSLNGEWRFAWFPAPAVPESWLECDLPEADTVVVPNSWQMHGYDAPIYTNVYPIVNPFPVPTENPTGCYSLTFNVDESWLQEQQTRIFD  
GVNSAFHLWCNGRWVYGYQDSRLPSEFDLSAFLRAGENRLAVMVLRWSDGSYLEDDQDMWRMSGIFRDVSLHLKPTTQISDFHVATRNDDFS  
AVLEAEVQMCGERLDYLRVTVSLWQGETQVASGTAPFGGEIIDERGGYADRVTLRLNVENPKLWSAEIPNLRYAVVELHTADGTLIEAEACDVGR  
EVDRIENGLLLLNGKPLLIRGVNRHEHPLHGQVMDEQTMVQDILLMKQNNFNAVRCSHYPNHPLWYTLCDRYGLYVDEANIETHGMVPMNRL  
TDDPRWLPAMSERVTRMVQRDRNHPVIVSLGNESGHGANHDALYRWIKSVDPSPVQYEGGADTTATDIICPMYARVDEDQPPFAVPKWS  
IKKWLSPGETRPLILCEYAHAMGNSLGGFAKYWQAFRQYPRLQGGFVWDVVDQSLIKYDENGPNWSAYGGDFGDTPNDRQFCMNGLVFADR  
TPHPALTEAKHQQQFFQRLSGQTIETVSEYLFHRHSDNELLHWMVALDGGKPLASGEVPLDVAPQGGKQIHELPELPQESAGQLWLTVRVVQPNATA  
WSEAGHISAWQQWRLAENLSVTLPAASHAIPHLTTSEMDFCIELGNKRWQFNRSQSGFLSQMWIGDKQLLTPLRDQFTRAPLNDIGVSEATR  
IDPNAWVERWKAAGHYQAEALLQCTADTLADAVLITTAHAWQHGGKTLFISRKYRIDGSGQMAITVDVEVASDTPHARIGLNCQLAQAERVN  
WLGLGPQENYPDRLTAACFDRWDLPLSDMYTPYVFPSENGLRGCTRELNYGPHQWRGDFQFNISRYSQQLMETSHRHLLHAEETWLNIDGF  
HMGIGGDDSWSPVSAEFQLSAGRYHYQLVWCQK-

## METHODS

**Expression constructs.** All expression constructs were cloned using standard PCR methods and Gibson assembly. DNA fragments encoding antigens were ordered from Integrated DNA Technologies unless described otherwise. All inserts were authenticated using Sanger sequencing (Source BioScience). See Supplementary Table 1 for the amino acid sequences of all proteins expressed. pET28a-SpyCatcher-mi3 (GenBank MH425515, Addgene 112255) has been described<sup>[44]</sup>. pET28a-SpyCatcher003-mi3 (GenBank MT945417, Addgene 159995) was created by replacing SpyCatcher in pET28a-SpyCatcher-mi3 with SpyCatcher003<sup>[45]</sup>. pET28a-His<sub>6</sub>-Spy0469 (GenBank MT945418, Addgene 159996) was created by inserting a synthetic fragment encoding *S. pyogenes* (NS5496 strain) Spy0469 amino acids 24-389 into pET28a. pET28a-His<sub>6</sub>-PsaA (GenBank MT945419, Addgene 159997) was created by inserting a synthetic fragment encoding *S. pneumoniae* (GPSC5 strain) PsaA amino acids 19-309 into pET28a. pET28a-His<sub>6</sub>-SpyCatcher and pET28a-His<sub>6</sub>-SpyCatcher003 were created by inserting SpyCatcher (GenBank JQ478411)<sup>[46]</sup> or SpyCatcher003 (GenBank MN433887)<sup>[45]</sup> into pET28a. pET28a-His<sub>6</sub>-SnoopCatcher was created by inserting SnoopCatcher (GenBank KU500646)<sup>[47]</sup> into pET28a. pET28a-His<sub>6</sub>-SUMO-SnoopTagJr (GenBank MT945420) was created by inserting *Saccharomyces cerevisiae* Small Ubiquitin-like Modifier (SUMO) protein (GenBank NM001180818) and SnoopTagJr (KLGSIIEFIKVNK)<sup>[48]</sup> into pET28a. pET28a-His<sub>6</sub>-SpyTag003-OspC (GenBank MT945421, Addgene 159998) was created by inserting His<sub>6</sub> tag, GSGESG linker, SpyTag003 (RGVPHIVMVDAYKRYK)<sup>[45]</sup> and *B. burgdorferi* N40 strain OspC (GenBank JN969070) amino acids 20-209 with C129S substitution, into pET28a. The C129S substitution was made to prevent OspC aggregation as previously described<sup>[49]</sup>. pET28a-His<sub>6</sub>-SpyTag003- $\beta$ -galactosidase was a kind gift from Juha Huiskonen, University of Helsinki, and contains His<sub>6</sub> tag, GSGESG linker, SpyTag003 and *E. coli*  $\beta$ -galactosidase amino acids 1-1024 cloned into pET28a. For streptavidin, we used the pET21-DTag construct (streptavidin bearing SpyTag at its C-terminus, with mutations reducing biotin-binding affinity) (GenBank KJ906520, Addgene ID 59548), which has been described<sup>[50]</sup>. pcDNA3.1-H3Vic-SpyTag003-His<sub>6</sub> (GenBank MT945422) was created by inserting Influenza A/Victoria/361/2011 H3 (GenBank KJ942680) amino acids 1-521 (synthesized by GeneArt), GSGSGSPGS linker, T4 bacteriophage fibritin foldon domain, (GSG)<sub>3</sub> linker, SpyTag003 and His<sub>6</sub> tag into pcDNA3.1. pcDNA3.1-H3Aichi-SpyTag003-His<sub>6</sub> (GenBank MT945423) was created in the same way using Influenza A/Aichi/2/1968 (GenBank EF614251) H3 coding sequence. The expression constructs for both H3 variants lack the natural 5' and 3' untranslated regions (UTRs) and the transmembrane domain. pcDNA3.1-His<sub>6</sub>-SpyTag-VASP-N1 (GenBank MT945424) was created by cloning Influenza A/PR/8/1934 H1 signal sequence, His<sub>6</sub> tag, SSSGSG linker, SpyTag (AHIVMVDAYKPTK), (GSG)<sub>3</sub> linker, human Vasodilator-stimulated phosphoprotein (VASP) tetramerization domain (GenBank NM003370.4) amino acids 338-375 and Influenza A/England/195/2009 N1 (GenBank ACR15621) amino acids 69-469 (synthesized by GeneArt) into pcDNA3.1. pcDNA3.1-His<sub>6</sub>-SpyTag-VASP-N2 (GenBank MT945425) was created in the same way using Influenza A/Victoria/361/2011 N2 (GenBank KJ942682) amino acids 68-469. The expression constructs for both N1 and N2 lack the natural 5' and 3' UTRs and the transmembrane domain. pcDNA3.1-SpyTag-RBD (GenBank MT945427, Addgene 159999) was created by cloning Influenza A/Guangdong/2017 H7 signal sequence, SpyTag, (GSG)<sub>3</sub> linker and SARS-CoV-2 spike glycoprotein (GenBank NC045512) amino acids 340-538 (synthesized by GeneArt) into pcDNA3.1. pHL-sec-NDV-HN-SpyTag-His<sub>6</sub> (GenBank MT945426, Addgene 160000) has the following organization in the pHL-sec backbone: chicken receptor tyrosine phosphatase  $\alpha$  signal sequence, Avian avulavirus Kansas strain HN protein (GenBank AF212323) amino acids 47-575, (GGG)<sub>3</sub> linker, SpyTag,

GSGGTK linker, His<sub>6</sub>. Vectors for His<sub>6</sub>-tagged SUMO protease Ulp1<sup>[51]</sup> and His<sub>6</sub>-MBP-TEV protease<sup>[52]</sup> have been described.

**Expression and purification of SpyCatcher003-mi3.** SpyCatcher003-mi3 was expressed in *E. coli* BL21(DE3) RIPL cells (Agilent). Heat-shock transformed cells were plated on LB-Agar plates with 50 µg/mL kanamycin and incubated for 16 h at 37 °C. A single colony was picked into 10 mL starter culture of LB media with 50 µg/mL kanamycin, and incubated for 16 h at 37 °C with shaking at 200 rpm. The pre-culture was diluted 1:100 into 1 L LB supplemented with 50 µg/mL kanamycin and 0.8% (w/v) glucose and cultured at 37 °C, 200 rpm until OD<sub>600</sub> = 0.6. Protein expression was induced with 420 µM isopropyl β-D-1-thiogalactopyranoside (IPTG) and incubation was continued at 22 °C, 200 rpm for 16 h. The cell pellet from 500 mL culture was resuspended in 20 mL 25 mM Tris-HCl, 300 mM NaCl, pH 8.5, supplemented with 0.1 mg/mL lysozyme, 1 mg/mL cOmplete mini EDTA-free protease inhibitor (Merck) and 1 mM phenylmethanesulfonyl fluoride (PMSF). Cell suspension was incubated at 22 °C for 30 min on a platform shaker and sonicated on ice 4 times for 60 s at 50% duty-cycle using an Ultrasonic Processor (Cole-Parmer) equipped with a microtip. Cell lysate was clarified by centrifugation at 35,000 g for 45 min at 4 °C. The supernatant was filtered through both 0.45 µm and 0.22 µm syringe filters (STARLAB) and 170 mg ammonium sulfate was added per mL of lysate. SpyCatcher003-mi3 particles were precipitated by incubating the lysate at 4 °C for 1 h while mixing at 100 rpm with a magnetic stirrer. Precipitated particles were pelleted by centrifugation at 30,000 g for 30 min at 4 °C. Supernatant was discarded and the pellet was resuspended into 8 mL 25 mM Tris-HCl, 150 mM NaCl, pH 8.5. Residual ammonium sulfate was removed by dialyzing for 16 h against 500-fold excess of the same buffer. Dialyzed SpyCatcher003-mi3 was centrifuged at 17,000 g for 30 min at 4 °C to pellet any insoluble material. The supernatant was filtered through a 0.22 µm syringe filter to further remove insoluble material. 2.5 mL was loaded into a HiPrep Sephacryl S-400 HR 16-600 SEC column (GE Healthcare) equilibrated with 25 mM Tris-HCl, 150 mM NaCl, pH 8.5 using an ÄKTA Pure 25 system (GE Healthcare). Proteins were separated at 1 mL/min while collecting 1 mL elution fractions. The fractions containing the purified particles were identified by SDS-PAGE, pooled, and concentrated using a Vivaspin 20 100 kDa M<sub>w</sub> cut-off spin concentrator. Endotoxin was removed from the SpyCatcher003-mi3 samples using Triton X-114 phase separation as previously described<sup>[52]</sup>. Briefly, 1% (v/v) Triton X-114 was added to SpyCatcher003-mi3 samples and the solution was mixed by gentle pipetting. The samples were incubated on ice for 15 min or until Triton X-114 had completely dissolved. The tubes were transferred to a 37 °C water bath and incubated for 5 min. Micellar Triton X-114 was separated by centrifugation at 16,900 g for 5 min at 30 °C and the top phase was carefully separated into a fresh endotoxin-free microcentrifuge tube. Triton X-114 phase separation was repeated twice more. After the third round, residual Triton X-114 was removed by an additional incubation at 37 °C for 5 min, followed by centrifugation at 16,900 g for 10 min at 30 °C. The concentration of endotoxin-depleted particles was measured using bicinchoninic acid (BCA) assay (Pierce) and particles were stored at -80 °C. Estimated yield per L culture was calculated based on a purification using 250 mL of cell suspension. VLP sample purity was estimated using SDS-PAGE and gel densitometry.

**Expression and purification of OspC and β-galactosidase.** SpyTag003-OspC and SpyTag003-β-galactosidase were expressed in *E. coli* BL21(DE3) RIPL cells (Agilent). 5 mL overnight cultures were diluted into 1 L LB supplemented with 50 µg/mL kanamycin and 0.8% (w/v) glucose. Cultures were incubated at 37 °C, 200 rpm until OD<sub>600</sub> = 0.5 and protein expression was induced with 840 µM IPTG for β-galactosidase or 420 µM IPTG for OspC. Incubation was continued for 3 h at 37 °C, 200 rpm for β-galactosidase and 3 h at 30 °C, 200

rpm for OspC. Cell pellets from 1 L cultures were resuspended into 20 mL ( $\beta$ -galactosidase) or 15 mL (OspC) of 50 mM Tris-HCl pH 7.8, 300 mM NaCl supplemented with 0.1 mg/mL lysozyme, 1 mg/mL cOmplete mini EDTA-free protease inhibitor and 1 mM PMSF.  $\beta$ -galactosidase lysis buffer was supplemented with 2 mM 2-mercaptoethanol and OspC lysis buffer with 10 mM imidazole. Cells were lysed by incubation for 1 h at 4 °C on a roller shaker, followed by sonication on ice 4 times for 60 s each at 50% duty-cycle using an Ultrasonic Processor (Cole-Parmer) equipped with a microtip. Cell debris was pelleted by centrifugation at 35,000 g for 45 min at 4 °C and the supernatant was mixed with 1 mL Ni-NTA sepharose (Qiagen) equilibrated with the lysis buffer. After 30 min incubation at 4 °C on a roller shaker, the mixtures were added to gravity-driven Econo-Pac polypropylene columns (Bio-Rad) and resin was washed with 15 column volumes (CV) of lysis buffer, followed by 15 CV of lysis buffer with 10 mM imidazole and then 5 CV of lysis buffer with 30 mM imidazole. Bound proteins were eluted by 200 mM imidazole in the lysis buffer and imidazole was removed by dialysis for 16 h using 3.5 kDa Spectra/Por-3 dialysis membrane (Spectrum Chemical). SpyTag003- $\beta$ -galactosidase was dialyzed once against 25 mM Tris-HCl pH 7.5, 150 mM NaCl, 5 mM EDTA, 2 mM tris(2-carboxyethyl)phosphine (TCEP), followed by dialyzing twice against 25 mM Tris-HCl pH 7.5, 150 mM NaCl, 2 mM MgCl<sub>2</sub>, 2 mM CaCl<sub>2</sub>, 2 mM TCEP. SpyTag003-OspC was dialyzed once against 25 mM Tris-HCl pH 7.5, 150 mM NaCl, 5 mM EDTA and twice against 25 mM Tris-HCl pH 7.5, 150 mM NaCl. Dialyzed proteins were concentrated using VivaSpin spin concentrators with 100 kDa cut-off for  $\beta$ -galactosidase and 30 kDa cut-off for OspC. Concentrated proteins were further purified using an ÄKTA Pure 25 (GE Life Sciences) and size exclusion columns. For both proteins, the last dialysis buffer was used as the moving phase. SpyTag003- $\beta$ -galactosidase was purified using Superose 6 Increase 10-300 column (GE Life Sciences) at 0.75 mL/min. SpyTag003-OspC was purified using a HiLoad Superdex 75pg 16-600 column (GE Life Sciences) at 1 mL/min. Purified proteins were concentrated using the same spin concentrators as before and stored at -80 °C. The final yields per L of culture medium were 3.4 mg for SpyTag003-OspC and 1.5 mg for SpyTag003- $\beta$ -galactosidase.

**Expression and purification of Streptavidin-SpyTag fusion.** Dead Streptavidin-SpyTag homotetramer was expressed in *E. coli* BL21(DE3) RIPL cells (Agilent) and purified from inclusion bodies as previously described<sup>[50]</sup>. Briefly, 15 mL overnight cultures were diluted into 1 L LB supplemented with 100  $\mu$ g/mL ampicillin and 0.8% (w/v) glucose. Cultures were incubated at 37 °C, 200 rpm until OD<sub>600</sub> = 0.6 and protein expression was induced with 420  $\mu$ M IPTG. Incubation was continued for 4 h at 37 °C, 200 rpm. Cell pellets from 1 L cultures were resuspended into 15 mL PBS (137 mM NaCl, 2.7 mM KCl, 10 mM Na<sub>2</sub>HPO<sub>4</sub>, 1.7 mM KH<sub>2</sub>PO<sub>4</sub>, pH 7.4), supplemented with 1% (v/v) Triton X-100, 0.1 mg/mL lysozyme, 1 mg/mL cOmplete mini EDTA-free protease inhibitor, 1 mM PMSF and 10 mM EDTA. Cells were lysed by incubation for 30 min at 22 °C on a platform shaker, followed by sonication on ice 3 times for 60 s each at 50% duty-cycle using an Ultrasonic Processor (Cole-Parmer) equipped with a microtip. Insoluble material was pelleted by centrifugation at 27,000 g for 20 min at 4 °C, the supernatant discarded and the pellet containing streptavidin inclusion bodies carefully resuspended in 10 mL PBS supplemented with 1% (v/v) Triton X-100, 1 mg/mL cOmplete mini EDTA-free protease inhibitor, 1 mM PMSF and 10 mM EDTA. The mixture was diluted with additional 20 mL of the same buffer and centrifuged at 27,000 g for 20 min at 4 °C. The inclusion bodies were washed three more times, each time resuspending the pellet into 30 mL PBS supplemented with 10 mM EDTA. The final pellet was resuspended into 6 mL 6 M guanidinium hydrochloride pH 1.5 and any remaining solid material pelleted by centrifugation at 27,000 g for 30 min at 4 °C. For streptavidin refolding, the supernatant was left to slowly drip through a 10  $\mu$ L pipet tip into 250 mL ice cold PBS with 10 mM EDTA mixed at high

speed on a magnetic stirrer. The mixing speed was lowered to 150 rpm and the solution left to mix for 16 h at 4 °C. Any insoluble material was removed by filtration through cellulose filter paper (Whatman) and the streptavidin tetramers in the flow-through were precipitated with 150 g ammonium sulfate per 250 mL PBS (60% of the saturation point at 4 °C). The mixture was incubated for 2 h with gentle mixing and the precipitate was pelleted by centrifugation at 20,000 g for 30 min at 4 °C. The supernatant was discarded and the pellet dissolved into 15 mL 25 mM Tris-HCl, 150 mM NaCl, 5 mM EDTA pH 8.0 and dialyzed twice against the same buffer. Any precipitated material was pelleted by centrifugation at 4,500 g for 10 min at 4 °C. The refolded streptavidin was further purified using 2-iminobiotin affinity chromatography. The protein sample was added to a 1 mL column of 2-iminobiotin agarose resin (Affiland) pre-equilibrated with 50 mM sodium borate, 500 mM NaCl, pH 10.0 (binding buffer). The column was left to empty by gravity flow and the resin was washed twice with 15 CV of the binding buffer. Resin-bound streptavidin was eluted with 15 CV of 20 mM NaH<sub>2</sub>PO<sub>4</sub> pH 2.0, collecting 1 mL fractions into microcentrifuge tubes containing 100 µL 1 M Tris-HCl, pH 8.0. Pooled elution fractions were dialyzed against PBS and concentrated using a VivaSpin 20 30 kDa spin filter.

**Expression and purification of Influenza antigens and NDV HN.** Influenza antigens and NDV HN were expressed in Expi293F cells (Thermo Fisher) following manufacturer's recommendations. Briefly, Expi293F cells were cultured in a humidified Multitron Cell incubator (Infors HT) at 37 °C with 8% (v/v) CO<sub>2</sub>, rotating at 125 rpm, for at least 3 passages before transient transfection. Cells were transfected at  $2.5 \times 10^6$  cells/mL using 2.7 µL ExpiFectamine 293 (Thermo Fisher) and 1 µg endotoxin-free plasmid DNA per 1 mL of cell suspension. All proteins were expressed at 60 mL total culture volume in vented 250 mL shake flasks (Corning). Transfection enhancers 1 and 2 (Thermo Fisher) were added 18 h post-transfection and culture continued until cell viability dropped under 40-60% (4-6 days post-transfection). Proteins were purified from cell culture supernatants using Ni-NTA-sepharose and SEC. Briefly, cell culture supernatants were clarified by centrifugation at 3,500 g for 5 min at 22 °C, followed by filtration through a 0.22 µm syringe filter. Cleared supernatants were mixed with one quarter supernatant volume of 50 mM Tris-HCl pH 8.0, 300 mM NaCl. For H3, N1 and N2, 10 mM imidazole was added to the supernatants and the pH adjusted to 8.0 using 0.1 M NaOH. The supernatants were mixed with 0.75-1.5 mL Ni-NTA-sepharose (Qiagen) pre-equilibrated with 50 mM Tris-HCl pH 8.0, 300 mM NaCl and the mixtures were incubated on a roller shaker for 1 h at 4 °C. The mixtures were loaded into polypropylene columns and washed with 10 CV of 10 mM imidazole in 50 mM Tris-HCl pH 8.0, 300 mM NaCl and then 5 CV of 30 mM imidazole in 50 mM Tris-HCl pH 8.0, 300 mM NaCl. Proteins were eluted with 200 mM imidazole in 50 mM Tris-HCl pH 8.0, 300 mM NaCl. H3 Vic, H3 Aichi, N1 and N2 were dialyzed against 25 mM Tris-HCl pH 8.0, 150 mM NaCl, 10 mM EDTA. NDV HN was dialyzed against 25 mM Tris-HCl pH 8.0, 150 mM NaCl. All proteins were concentrated with VivaSpin 20 30 kDa spin filters and further purified using SEC. H3 Vic and H3 Aichi were purified using Superose 6 increase 10-300 column (GE Life Sciences) equilibrated with 25 mM Tris-HCl pH 8.0, 150 mM NaCl at 0.75 mL/min flow rate. N1 and N2 were purified using the same column equilibrated with 25 mM Tris-HCl pH 8.0, 150 mM NaCl, 2 mM CaCl<sub>2</sub> at 0.75 mL/min flow rate. NDV HN was purified using HiLoad Superdex 200pg 16-600 column (GE Life Sciences) equilibrated with 25 mM Tris-HCl pH 8.0, 150 mM NaCl at 1.0 mL/min flow rate. Gel filtration standard (Bio-Rad 1511901) was run using the same parameters. The final yields per L of Expi293 medium (Thermo Fisher) were 63 mg for H3 Vic, 32 mg for H3 Aichi, 2.3 mg for N1, 28 mg for N2, and 44 mg for NDV HN.

**Expression and purification of SARS-CoV-2 RBD.** SARS-CoV-2 RBD was expressed in Expi293F cells using ExpiFectamine293 transfection reagent and transfection enhancers (Thermo Fisher) as described above. SpyTag-RBD was purified from cell culture supernatant using Spy&Go affinity purification with minor modifications<sup>[53]</sup>. Briefly, filtered cell-culture supernatants were diluted with one third supernatant volume of TP buffer (25 mM orthophosphoric acid adjusted to pH 7.0 at 22 °C with Tris base) and adjusted to pH 7.2. Spy&Go resin equilibrated with the same buffer was mixed with the diluted supernatant and incubated at 4 °C for 1 h with gentle stirring. The mixture was poured into an Econo-Pak column (Bio-Rad) and the column allowed to empty by gravity. The resin was washed with 2 × 10 CV of TP buffer. SpyTag-RBD was eluted with 2.5 M imidazole in TP buffer adjusted to pH 7.0 at 22 °C. Elution buffer was added 1 CV at a time and incubated with the resin for 5 min before collecting each fraction. Elution fractions were analyzed using SDS-PAGE with Coomassie staining and the fractions containing SpyTag-RBD were pooled and dialyzed against 10 mM Tris-HCl pH 8.0, 200 mM NaCl. The sample was concentrated using Vivaspinn-20 10 kDa and further purified using ÄKTA Pure 25 (GE Life Sciences) equipped with Superdex 75pg 16-600 column (GE Life Sciences), run at 1 mL/min. The dialysis buffer was used as the moving phase. The final yield of purified SpyTag-RBD per L of Expi293 medium was 99.6 mg.

**Expression, purification and conjugation of antigens for human sero-reactivity ELISA.** His<sub>6</sub>-SpyCatcher, His<sub>6</sub>-SpyCatcher003, His<sub>6</sub>-SnoopCatcher, His<sub>6</sub>-SUMO-SnoopTagJr, His<sub>6</sub>-Spy0469 and His<sub>6</sub>-PsaA were expressed in *E. coli* BL21(DE3) RIPL cells as described above for SpyCatcher003-mi3 with minor modifications. Protein expression was induced at OD<sub>600</sub> = 0.5 with 420 μM IPTG and incubation was continued at 30 °C for 4 h. Cell pellets from 500 mL cultures were lysed in 50 mM Tris-HCl pH 7.8, 300 mM NaCl supplemented with 10 mM imidazole, the lysate was cleared by centrifugation, and the cleared lysate was loaded into gravity-driven polypropylene columns with Ni-NTA-sepharose (Qiagen) pre-equilibrated with the lysis buffer. Resin was washed 5 times with 10 CV of 50 mM Tris-HCl pH 7.8, 300 mM NaCl containing 10 mM imidazole and twice with 1 CV of 50 mM Tris-HCl pH 7.8, 300 mM NaCl with 30 mM imidazole. Bound proteins were eluted by 200 mM imidazole in 50 mM Tris-HCl pH 7.8, 300 mM NaCl and samples of each fraction were run on SDS-PAGE. Selected fractions were pooled and imidazole was removed by dialysis twice against 50 mM Tris-HCl pH 7.8, 300 mM NaCl. SnoopTagJr was released from His<sub>6</sub>-SUMO-SnoopTagJr by incubation with lab-made His<sub>6</sub>-tagged SUMO protease at 1:50 molar ratio for 13 h at 12 °C in the presence of 10% (v/v) glycerol. His-tags were removed from all other proteins by 16 h incubation at 4 °C with lab-made His<sub>6</sub>-MBP-TEV protease added at 1:25 molar ratio in 50 mM Tris-HCl, 0.5 mM EDTA, 1 mM dithiothreitol (DTT) pH 8.0. His<sub>6</sub>-MBP-TEV, His<sub>6</sub>-tagged SUMO protease and the cleaved His<sub>6</sub> fragments were removed by recapturing with Ni-NTA-sepharose resin. Proteins in the flow-through were dialyzed against 50 mM Tris-HCl pH 8.5, 150 mM NaCl and stored at -80 °C.

Before human sero-reactivity ELISA, 50 μM SpyCatcher (cleaved with His<sub>6</sub>-MBP-TEV protease) was reacted in PBS with two-fold molar excess of solid-phase synthesized SpyTag peptide (GAHIVMVDAYKPTK, 98% purity, Insight Biotechnology). 50 μM SpyCatcher003 cleaved with TEV protease was reacted in PBS with two-fold molar excess of solid phase-synthesized SpyTag003 peptide (RGVPHIVMVDAYKRYK, 95% purity, Insight Biotechnology). After 2 h incubation at 22 °C, excess Tags were removed by dialyzing three times against PBS pH 7.5 using 7 kDa M<sub>w</sub> cut-off SnakeSkin dialysis tubing (Thermo Fisher). TEV protease-cleaved SnoopCatcher was reacted in 50 mM sodium borate pH 10.0 with 2-fold molar excess of SnoopTagJr peptide (GKLGSIIEFIKVNKGS) generated by SUMO protease-cleavage of His<sub>6</sub>-SUMO-SnoopTagJr as described above. SnoopCatcher and SnoopTagJr were

incubated for 16 h at 22 °C and excess SnoopTagJr was removed by repeated washing in a Vivaspin 500 spin column with 5 kDa  $M_w$  cut-off membrane. Complete Tag:Catcher conjugation and successful removal of excess tags were confirmed using SDS-PAGE with Coomassie staining.

**Human sero-reactivity ELISA.** For indirect ELISA, Maxisorp F96 plates (Nunc) were coated for 16 h at 4 °C with 100  $\mu$ L 2  $\mu$ g/mL of antigens diluted in PBS. Wells were washed 6 times with PBS supplemented with 0.05% (v/v) Tween-20 (PBS-T) and blocked with 300  $\mu$ L Blocker Casein in PBS (Thermo Fisher) for 1 h at 22 °C, after which the wash with PBS-T was repeated. Serum samples were serially diluted into the blocking buffer using 7-point, 4-fold series starting at 1:100. 50  $\mu$ L of serum samples were added per well and incubated for 2 h at 22 °C. Wells were washed 6 times with PBS-T and 50  $\mu$ L alkaline phosphatase conjugated anti-human IgG antibody (Sigma-Aldrich A1543) diluted 1:1,000 in the blocking buffer was added to each well. After 1 h incubation at 22 °C, wells were washed 6 times with PBS-T with 3 min incubations at each wash. After the final wash, excess buffer was carefully removed by tapping the plates on paper towels. 100  $\mu$ L 1 mg/mL para-nitrophenyl phosphate (pNPP) substrate (Sigma-Aldrich) diluted in 1 M diethanolamine (pH 9.8) was added to each well. OD<sub>405</sub> was measured at 30 s intervals for 30 min using a Tecan Infinite F50 plate reader. To minimize plate-to-plate variation, control wells on all plates were coated with Spy0469 and incubated with a pool of 10 serum samples diluted 1:100. OD<sub>405</sub> of these control wells was used to determine plate-specific time-points for data analysis. To correct for antigen-specific background caused by any non-specific binding of the secondary antibody, the mean OD<sub>405</sub> of antigen-coated blank wells was subtracted from OD<sub>405</sub> of wells incubated with serum samples. To correct for sample-specific background, each serum dilution was incubated on non-coated control wells and the blank-corrected OD<sub>405</sub> from these wells was subtracted from OD<sub>405</sub> of all antigen-coated wells incubated with the matching serum dilution. Endpoint dilution was defined as the intersection of the dilution curve and the horizontal line at OD<sub>450</sub> = mean + 5 $\times$  s.d. of antigen-coated blank wells. For correlation analysis of endpoint values, Pearson correlation coefficient was calculated in GraphPad Prism 7 (GraphPad software) using log<sub>10</sub>-transformed endpoint titers. Linear regression lines were fitted to the endpoint titers in GraphPad Prism 7 (GraphPad software) for data visualization.

For sandwich ELISA, Maxisorp F96 plates (Nunc) were coated for 16 h at 4 °C with 100  $\mu$ L anti-His<sub>6</sub> antibody (Qiagen 34660) diluted to 0.3  $\mu$ g/mL in PBS. Wells were washed 6 times with PBS-T, blocked with Blocker Casein in PBS (Thermo Fisher) and 100  $\mu$ L of SpyTag:SpyCatcher, SpyTag:His<sub>6</sub>-SpyCatcher, SpyTag003:SpyCatcher003 or SpyTag003:His<sub>6</sub>-SpyCatcher003 at 2  $\mu$ g/mL in the blocking buffer were added to each well. Plates were incubated for 1 h at 22 °C and washed with PBS-T as above. 50  $\mu$ L of human serum samples diluted 1:100 in the blocking buffer were added to each well and plates were incubated for 2 h at 22 °C. The presence of SpyTag:SpyCatcher-specific antibodies was detected using alkaline phosphatase conjugated anti-human IgG antibody (Sigma-Aldrich, A1543) and pNPP substrate (Sigma-Aldrich) as described above for endpoint ELISA. To correct for sample-to-sample variance in non-specific binding, OD<sub>405</sub> of control wells coated with anti-His<sub>6</sub> antibody and incubated with tagless SpyTag:SpyCatcher or tagless SpyTag003:SpyCatcher003 was subtracted from OD<sub>405</sub> of the wells coated with anti-His<sub>6</sub> antibody and incubated with SpyTag:His<sub>6</sub>-SpyCatcher or SpyTag003:His<sub>6</sub>-SpyCatcher003, respectively.

The study was conducted according to the principles of the Declaration of Helsinki and in accordance with Good Clinical Practice (GCP). The analyzed samples were collected from healthy UK adults as a part of the VAC063 study (Clinicaltrials.gov identifier NCT02927145), University of Oxford, and used where informed, signed consent by the donor covered further use of the samples in vaccine research. The VAC063 study received ethical approval from the

UK NHS Research Ethics Service (Oxfordshire Research Ethics Committee A, Ref 16/SC/0345).

**VLP thermal stability assay.** To analyze VLP thermal stability, 50  $\mu\text{L}$  aliquots of SpyCatcher-mi3 or SpyCatcher003-mi3 at 30  $\mu\text{M}$  in 25 mM Tris-HCl, 150 mM NaCl, pH 8.5 were incubated at 25 °C, 37 °C, 55 °C, 75 °C or 95 °C for 60 min and cooled to 4 °C for 10 min using a Thermal Cycler C1000 (Bio-Rad). Following incubation, aggregates were removed by centrifugation at 16,900 g for 30 min at 4 °C. Samples of supernatant were resolved on 16% SDS-PAGE stained with InstantBlue Coomassie (Expedion) and imaged using a ChemiDoc XRS imager. The relative amount of soluble protein was analyzed using gel densitometry in ImageLab (version 5.2) software (Bio-Rad). The mean band intensities for samples incubated at 37 °C, 55 °C, 75 °C or 95 °C were normalized by dividing by the mean band intensity of samples incubated at 25 °C. All samples were analyzed in triplicate and plotted as mean  $\pm$  1 standard deviation.

**VLP:antigen conjugation and solubility assay.** Antigens at 2  $\mu\text{M}$ , 3  $\mu\text{M}$ , 4  $\mu\text{M}$  or 6  $\mu\text{M}$  were conjugated with 2  $\mu\text{M}$  SpyCatcher003-mi3. SARS-CoV-2 RBD, OspC, NDV HN, H3 Vic and N2 were conjugated in 25 mM Tris-HCl, 150 mM NaCl, pH 8.0. H3 Aichi was conjugated in 25 mM Tris-HCl, 620 mM NaCl, pH 8.0. N1 was conjugated in 25 mM Tris-HCl, 150 mM NaCl, 2 mM EDTA, pH 8.0.  $\beta$ -galactosidase was conjugated in 25 mM Tris-HCl, 620 mM NaCl, 10 mM TCEP, pH 8.0. All conjugations were incubated at 4 °C for 16 h and possible aggregates removed by centrifugation at 16,900 g for 30 min at 4 °C. Samples of the supernatant were mixed with reducing 6 $\times$  loading dye [0.23 M Tris-HCl, pH 6.8, 24% (v/v) glycerol, 120  $\mu\text{M}$  bromophenol blue, 0.23 M SDS, 0.2 M dithiothreitol] and resolved on 12%, 14% or 16% SDS-PAGE using the XCell SureLock system (Thermo Fisher). Gels were stained with InstantBlue Coomassie (Expedion) and imaged using a ChemiDoc XRS imager (Bio-Rad). The intensities of bands on each lane were quantified using ImageLab (version 5.2) software (Bio-Rad) and Fiji distribution of ImageJ (version 1.51n). For each antigen, the mean intensities of all bands were normalized by dividing by the mean intensity of non-conjugated SpyCatcher003-mi3 resolved at 2  $\mu\text{M}$  on the same gel. The normalized intensities of all bands on a single lane were plotted as stacked columns. Samples were analyzed in triplicate and plotted as mean  $\pm$  1 standard deviation.

For the solubility analysis of antigen-decorated VLPs, antigens were conjugated with SpyCatcher003-mi3 VLP at 1:1 molar ratio as described above. After conjugation, total protein samples were mixed with reducing 6 $\times$  loading dye and resolved on 12-16% SDS-PAGE without removing possible VLP aggregates. Soluble protein samples were centrifuged at 16,900 g for 30 min at 4 °C to pellet any aggregates and the supernatants were resolved on 12-16% SDS-PAGE in the same way as total protein samples. Gel densitometry was used to determine the band intensity of non-coupled SpyCatcher003-mi3 on each lane as described above. Soluble protein fraction for each antigen-VLP conjugate was defined as the ratio of mean SpyCatcher003-mi3 band intensity for the soluble protein sample divided by the mean band intensity for the total protein sample. All samples were analyzed in triplicate and plotted as mean  $\pm$  1 standard deviation.

**Dynamic Light Scattering (DLS).** SpyTag-antigens were conjugated at 1:1 molar ratio with 2  $\mu\text{M}$  SpyCatcher003-mi3 as described above. Samples were centrifuged for 30 min at 16,900 g at 4 °C to pellet possible aggregates and 30  $\mu\text{L}$  was loaded into a quartz cuvette. Before each measurement, the cuvette was incubated in the instrument for 5 min to allow sample temperature to stabilize. All samples were measured at 20 °C using an Omnisizer (Viscotek) with 20 scans of 10 s each using 50% laser intensity, 15% maximum baseline drift and 20%

spike tolerance. The intensity of the size distribution was normalized to the peak value and plotted in GraphPad Prism 7 (GraphPad Software).

**Thermofluor assay.** SpyTag003-OspC or NDV HN-SpyTag were conjugated with SpyCatcher003-mi3 for 4 h at 22 °C, using both antigens and VLP each at 15 µM monomer concentration. Remaining non-reacted SpyCatcher003 on the particles was blocked by adding solid-phase synthesized SpyTag003 peptide (Insight Biotechnology) at 22.5 µM for 2 h at 22 °C. Non-conjugated antigens and excess peptides were removed by dialysis against PBS pH 7.8 for 16 h at 4 °C using dialysis membrane with 1 MDa  $M_w$  cut-off (Spectrum Chemical). Control samples with free antigens were not incubated with free SpyTag003 but were dialyzed against the same buffer using dialysis membrane with 3.5 kDa  $M_w$  cut-off (Spectrum Chemical). Possible aggregates were removed by centrifugation for 30 min at 16,900 g at 4 °C and protein concentration was determined using BCA assay (Pierce). A negative control containing non-decorated SpyCatcher003-mi3 was incubated with SpyTag003 and dialyzed as described above. All samples were diluted with PBS pH 7.8 to 2.5 µM protein concentration and mixed with 5× SYPRO Orange (Thermo Fisher) in 50 µL. Samples were heated in an Mx3005P thermal cycler (Agilent) using 30 s at 25 °C, temperature ramping at 0.5 °C increments every 30 s for 150 rounds, and 30 s at 25 °C. SYPRO Orange fluorescence intensity was measured after each round using 492 nm excitation and 610 nm emission filters. The raw intensity values of SpyCatcher003-mi3 were subtracted from the values of antigen-decorated particles. Values of buffer controls with 5× SYPRO Orange were subtracted from the values of free antigens. Sample  $T_m$  value was defined as the peak value of the first derivative of background-corrected fluorescence intensity. All samples were analyzed in triplicate.

**Transmission electron microscopy (TEM).** SpyTag-antigens were conjugated at 1:1 molar ratio with 2 µM SpyCatcher003-mi3 as described above. Samples were centrifuged for 30 min at 16,900 g at 4 °C and diluted 1:5 using 25 mM Tris-HCl, 150 mM NaCl, pH 8.0. Protein samples were applied to glow-discharged carbon 200 mesh copper grids for 2 min and blotted with filter paper. Samples were stained with 2% (w/v) uranyl acetate for 10 s, blotted and air-dried. Grids were imaged in a FEI Tecnai T12 transmission electron microscope at 120 kV using a Gatan US1000 CCD camera.

**Immunogen preparation for vaccination.** 3 µM H3 Vic-SpyTag003 was conjugated with 2 µM SpyCatcher003-mi3 in 25 mM Tris-HCl, pH 8.0, 150 mM NaCl. 3 µM H3 Aichi-SpyTag003 was conjugated with 2 µM SpyCatcher003-mi3 in 25 mM Tris-HCl, pH 8.0, 620 mM NaCl. 4 µM SpyTag-N1 was conjugated with 2 µM SpyCatcher003-mi3 in 25 mM Tris-HCl, pH 8.0, 150 mM NaCl, 2 mM EDTA. Reactions were incubated for 16 h at 4 °C and centrifuged for 30 min at 16,900 g at 4 °C. Matching non-conjugated control antigens were diluted in the same buffers and incubated and centrifuged in the same way. The concentration of each sample was determined using BCA assay (Pierce) and the immunogens diluted to 4 µg/mL antigen concentration. Recombinant H3 Vic and H3 Aichi immunogens were diluted using 25 mM Tris-HCl, 150 mM NaCl, pH 8.0. Recombinant N1 immunogens were diluted using 25 mM Tris-HCl, 150 mM NaCl, 1 mM  $CaCl_2$  pH 8.0. The endotoxin content of all recombinant antigens was measured using the Limulus amoebocyte lysate (LAL)-based Chromogenic Endotoxin Quantitation Kit (Thermo Fisher) following manufacturer's instructions. For all immunogens, measured endotoxin content was < 0.2 EU/mL. Immunogens were prepared within 2 days of mouse immunization and stored on ice. Before intramuscular (i.m.) immunization, immunogens were mixed 1:1 (25 µL + 25 µL) with AddaVax adjuvant (Invivogen).

**S-FLU and Influenza virus production.** Pseudotyped S-FLU viruses were generated with H1N1 A/Puerto Rico/8/34 virus (Cambridge strain) (PR8) backbone as previously described<sup>[54]</sup>. Briefly, the HA signal sequence in the HA viral RNA was deleted, and the HA gene replaced by a transgene encoding enhanced green fluorescent protein (eGFP) inserted in the same reading frame. The S-FLU pseudotyped with different surface HA was propagated in MDCK-SIAT1 cells (Madin-Darby Canine Kidney cells stably transfected with human 2,6-sialyltransferase, SIAT1) stably expressing the HA of choice using a lentiviral transduction system (MDCK-HA). Cells were maintained in D10 medium [Dulbecco's Modified Eagle Medium (DMEM) supplemented with 10% (v/v) fetal calf serum (Sigma-Aldrich, F9665), 2 mM glutamine, 100 U/mL penicillin and 100 µg/mL streptomycin]. In brief, S-FLU seed virus was produced via transient transfection in HEK293T using Lipofectamine 2000 (Thermo Fisher) as described<sup>[54]</sup> in the presence of 0.5 to 1 µg/mL tosyl phenylalanyl chloromethyl ketone (TPCK)-treated trypsin (Sigma-Aldrich, 4370285) in viral growth media (VGM; DMEM, 1% (w/v) bovine serum albumin (Sigma-Aldrich A0336), 10 mM HEPES buffer, penicillin (100 U/mL) and streptomycin (100 µg/mL)]<sup>[54]</sup>. Supernatant containing seed virus was then propagated in MDCK-HA in the presence of TPCK-Trypsin (0.5 to 1 µg/mL) for 48 h.

Seed virus of NYMC X217 (H3N2 A/Victoria/361/2011) Influenza virus was obtained from the National Institute for Biological Standards and Control (NIBSC, UK). X217 was propagated by infecting a monolayer of MDCK-SIAT1 with  $10^3$  -  $10^4$  infective units of X217 seed virus for 1 h before replacing with VGM containing 0.5-1 µg/mL TPCK-treated trypsin. Virus was harvested after 48 h.

S-FLU were quantified as 50% Culture Infectivity Dose (CID<sub>50</sub>) with slight modifications to the published protocol<sup>[55]</sup>. X217 was quantified as hemagglutination unit (HAU). Briefly, harvested supernatants containing S-FLU were titrated in 2-fold serial dilution in VGM across a flat-bottom 96-well plate seeded with  $3 \times 10^4$  MDCK-SIAT1 cells. The plate was incubated at 37 °C for 16 h and fixed with 10% neutral buffered formalin (Sigma-Aldrich). eGFP signal was then read using a CLARIOstar plate reader (BMG Labtech). The dilution of virus giving 50% fluorescence signal (EC<sub>50</sub>) was calculated by linear interpolation. CID<sub>50</sub>/mL was calculated as EC<sub>50</sub> dilution  $\times$  the number of cells per well ( $3 \times 10^4$ ). For HAU, X217 was diluted on two-fold dilution series in 50 µL PBS in V-bottomed 96-well plates in duplicates. 50 µL of 0.5% (v/v) human red blood cells (RBCs) in PBS were then added to each well and the plate was incubated at 22 °C for 30 min to 1 h. RBCs were obtained from donors within the MRC Weatherall Institute of Molecular Medicine and used according to the Best Practice Guidance set by University of Oxford Research Ethics Committee. HAU was reported as the reciprocal of the dilution of virus in the last well with complete hemagglutination.

**Mouse immunization and blood sampling.** Animal experiments were performed according to the UK Animals (Scientific Procedures) Act Project License (PBA43A2E4) and approved by the University of Oxford Local Ethical Review Body. C57BL/6 female mice (5 weeks old at the time of experiment) were obtained from Envigo. Mice were housed in accordance with the UK Home Office ethical and welfare guidelines and fed on standard chow and water *ad libitum*. Isoflurane (Abbott) anesthetized mice were immunized on day 0 and day 14 i.m. with 50 µL S-FLU viruses or 0.1 µg of recombinant antigens. S-FLU was used at  $2 \times 10^6$  CID<sub>50</sub> dose diluted in VGM. All recombinant antigens were matched to 0.1 µg antigen dose. Animals were routinely monitored at least twice weekly by observation and weighing. Sera samples were obtained on day 42 via cardiac puncture of humanely sacrificed mice. The collected whole blood in Microtainer SST tubes (BD) was allowed to clot at 22 °C for 1- 2 h before spinning down at 10,000 g for 10 min. The clarified sera were transferred to fresh tubes and stored at - 20 °C.

**ELISA binding of sera to H3 or N1 expressed on cells.** MDCK-SIAT1 cells ( $1 \times 10^4$ /well) were seeded in a 96-well U-bottomed plate two days before the assay. Next day wild-type Victoria/361/2011 virus (for H3 Vic expression), X31 H3N2 S-FLU (for H3 Aichi expression) or H7N1 S-FLU virus (for N1 expression) at multiplicity of infection  $\sim 1$  was added to the cells and incubated for 16 h. Serum samples were serially diluted in PBS + 0.1% (w/v) bovine serum albumin (dilution buffer) using 10-point, 2.5-fold series starting at 1:40. 50  $\mu$ L of serum samples were added to cells washed with PBS and incubated for 1 h at 22 °C. Cells were washed with PBS and 50  $\mu$ L horseradish-peroxidase (HRP) conjugated anti-mouse IgG antibody (Dako P0447) diluted 1:800 in the dilution buffer was added to each well. After 1 h incubation at 22 °C, wells were washed twice with PBS. The signal was then developed by adding BM Blue POD substrate (3,3'-5,5'-tetramethylbenzidine) (Roche 11484281001) for 5 min before stopping with 50  $\mu$ L of 1 M H<sub>2</sub>SO<sub>4</sub>. Plates were read at OD<sub>450</sub> using a CLARIOstar plate reader (BMG Labtech). Binding EC<sub>50</sub> was derived by linear interpolation from neighboring points in the titration curve. IC<sub>50</sub>/EC<sub>50</sub> ratio was calculated by dividing the log<sub>10</sub>-transformed IC<sub>50</sub> from the microneutralization assay or ELLA by the log<sub>10</sub>-transformed EC<sub>50</sub> from the cell-based titering. Samples with below-threshold titers in either assay were omitted from the analysis.

**Indirect ELISA for mouse sera.** 96-well MaxiSorp microtiter plates (Thermo Fisher) were coated for 16 h at 4 °C with 100  $\mu$ L recombinant Influenza antigens diluted to 5  $\mu$ g/mL in PBS. Plates were washed 6 times with PBS-T and blocked with PBS-T with 5% (w/v) skim milk for 1 h at 22 °C. Plates were washed 6 times with PBS-T and incubated with serum samples diluted in 1% (w/v) skim milk in PBS-T. All samples were diluted on a 2.5-fold, 12-point series starting at 1:40 dilution and analyzed in duplicate. Plates were washed 6 times with PBS-T and incubated for 1 h at 22 °C with 100  $\mu$ L of goat anti-mouse total IgG conjugated to alkaline phosphatase (Sigma-Aldrich, A3562) at 1:3,000 dilution in 1% (w/v) skim milk in PBS-T. The wells were washed 6 times in PBS-T with 3 min incubations at each wash. After the final wash, excess buffer was carefully removed by tapping the plates on paper towels. 100  $\mu$ L of 1 mg/mL pNPP substrate (Sigma-Aldrich) diluted in 1 M diethanolamine (pH 9.8), was added to each well. The reactions were stopped after 6 min by the addition of 25  $\mu$ L 3 M NaOH per well. Absorbance at 405 nm and 630 nm was measured using a FLUOstar Omega plate reader (BMG Labtech). 630 nm absorbance was subtracted from the 405 nm value to correct for well-specific background. To correct for antigen-specific background signal, the mean absorbance values of blank wells coated with recombinant antigens and incubated with secondary antibody were subtracted from the absorbance values of wells coated with the same antigen and incubated with serum samples. GraphPad Prism 7 (GraphPad Software) was used to obtain 4-parameter logistic fits to the background-corrected data and to calculate EC<sub>50</sub>.

**Microneutralization assays.** Microneutralization assays were performed as described previously<sup>[54]</sup> with minor modifications. Mice serum samples were heat-inactivated at 56 °C for 30 min. Sera were two-fold serially diluted in PBS starting at 1:40 dilution in a flat bottomed 96-well plate and incubated with virus for 2 h at 37 °C with 5% (v/v) CO<sub>2</sub> in a tissue culture incubator. The virus dilution used for the microneutralization assays was pre-determined by performing two-fold serial dilution on MDCK-SIAT1 cells. The highest dilution of the virus giving maximum plateau infection was chosen for use in the microneutralization assay. Indicator MDCK-SIAT1 cells ( $3 \times 10^4$  per well) were added to the sera and virus mixture and incubated for 16 h. The suppression of infection was measured on formalin-fixed cells by detecting eGFP (for S-FLU) or nucleoprotein (NP) (for wild-type viruses) using a fluorescence plate reader (CLARIOstar, BMG Labtech) as described above. For NP staining, cells were

permeabilized with PBS containing 0.5% (v/v) Triton X-100 and 20 mM glycine and stained with 1 µg/mL dilution of in-house produced anti-NP antibody 2-8C<sup>[54]</sup> biotinylated with EZ-Link Sulfo-NHS-LC-Biotinylation Kit (Thermo Fisher, 21335). The detection was performed through secondary Alexa Fluor 647-conjugated streptavidin (Thermo Fisher, S21374).

**Enzyme-linked Lectin Assay (ELLA).** ELLA assays were performed as previously described<sup>[56]</sup>. In brief, the two-fold serially-diluted heat-inactivated sera were incubated with pre-titrated A/England/195/2009 virus as the NA source for 1-2 h. The virus dilution for the assay was pre-determined by titrating to obtain at least 5-fold signal to noise ratio. The mixture was transferred to a Nunc Immunoassay ELISA plate (Thermo Fisher, 439454) pre-coated for at least 2 h with 25 µg/mL fetuin (Sigma-Aldrich, F3385). The plate was incubated for 18-20 h at 37 °C with 5% (v/v) CO<sub>2</sub> in a tissue culture incubator. The inhibition of NA enzymatic activity was detected by adding HRP-conjugated peanut agglutinin (Sigma-Aldrich, L7759) at 1 µg/mL after washing the plates 3 times with PBS and then developing with 50 µL o-phenylenediamine dihydrochloride (OPD) solution (Sigma-Aldrich, P9187). The enzymatic reaction was stopped after 5-15 min using 50 µL 1 M H<sub>2</sub>SO<sub>4</sub> and the absorbance was read at 492 nm using a CLARIOstar plate reader (BMG Labtech).

**Statistical analysis.** All statistical analyses were performed using GraphPad Prism 7 (GraphPad Software). Comparisons between two groups were made using two-tailed Student's t-test when data normal distribution was assumed and Mann-Whitney U test when normal distribution could not be assumed. For pairwise comparison of SpyTag:SpyCatcher and SpyTag003:SpyCatcher003 endpoint titers in Fig. 2, Wilcoxon matched-pairs signed rank test was used. For all immunological assays in Fig. 5, statistical analyses were performed on log<sub>10</sub>-transformed data using one-way ANOVA with Bonferroni correction. Pearson correlation coefficient (PCC) of log<sub>10</sub>-transformed data was used to analyze the correlations between the endpoint titers of SpyTag:SpyCatcher, SnoopTag:SnoopCatcher and Streptococcal control antigens in Fig. S2 and S3. In all statistical tests,  $p < 0.05$  was considered to be statistically significant.

**Structure visualization.** Protein structures were visualized in PyMOL version 2.2.2 (Schrödinger). Structural models are from the following PDB IDs: SpyTag:SpyCatcher 4MLI, SnoopTag:SnoopCatcher (RrgA D4 domain) 2WW8, RBD 6W41, OspC 1G5Z, NDV HN 3T1E, HA H3 4UO0, NA N1 2HTY, VASP tetramerization domain 1USE, β-galactosidase 6DRV. The SpyCatcher003-mi3 model is based on the previously published i3-01 model<sup>[57]</sup> and SpyTag:SpyCatcher PDB ID 4MLI, with the connecting linker modelled in PyMOL. To present antigens at the same scale, all antigens were rendered in PyMOL using orthoscopic view. A red sphere was added at the final main-chain atom where SpyTag or SpyTag003 was fused.

### Data availability

Amino acid sequences of SpyCatcher003-mi3 and all SpyTag-antigens are available in Table S1. The cDNA sequences of the used antigens are available in GenBank as described above under "Expression constructs". Enquiries for further information and request for resources and reagents should be directed to and will be fulfilled by the Lead Contacts, Mark Howarth or Alain Townsend: mark.howarth@bioch.ox.ac.uk, alain.townsend@imm.ox.ac.uk.

## REFERENCES

[44] T. U. J. Bruun, A.-M. C. Andersson, S. J. Draper, M. Howarth, *ACS Nano* **2018**, *12*,

- 8855–8866.
- [45] A. H. Keeble, P. Turkki, S. Stokes, I. N. A. Khairil Anuar, R. Rahikainen, V. P. Hytönen, M. Howarth, *Proc. Natl. Acad. Sci. U. S. A.* **2019**, *116*, 26523–26533.
  - [46] B. Zakeri, J. O. Fierer, E. Celik, E. C. Chittock, U. Schwarz-Linek, V. T. Moy, M. Howarth, *Proc. Natl. Acad. Sci.* **2012**, *109*, E690–E697.
  - [47] G. Veggiani, T. Nakamura, M. D. Brenner, R. V. Gayet, J. Yan, C. V. Robinson, M. Howarth, *Proc. Natl. Acad. Sci. U. S. A.* **2016**, *113*, 1202–1207.
  - [48] C. M. Buldun, J. X. Jean, M. R. Bedford, M. Howarth, *J. Am. Chem. Soc.* **2018**, *140*, 3008–3018.
  - [49] D. G. Edmondson, S. Prabhakaran, S. J. Norris, A. J. Ullmann, J. Piesman, M. Dolan, C. Probst, C. Radzimski, W. Sticker, L. Komorowski, *Clin. Vaccine Immunol.* **2017**, *24*, e00306-16.
  - [50] M. Fairhead, G. Veggiani, M. Lever, J. Yan, D. Mesner, C. V. Robinson, O. Dushek, P. A. van der Merwe, M. Howarth, *J. Am. Chem. Soc.* **2014**, *136*, 12355–12363.
  - [51] R. Assenberg, O. Delmas, S. C. Graham, A. Verma, N. Berrow, D. I. Stuart, R. J. Owens, H. Bourhy, J. M. Grimes, *Acta Crystallogr. Sect. F Struct. Biol. Cryst. Commun.* **2008**, *64*, 258–262.
  - [52] K. D. Brune, D. B. Leneghan, I. J. Brian, A. S. Ishizuka, M. F. Bachmann, S. J. Draper, S. Biswas, M. Howarth, *Sci. Rep.* **2016**, *6*, 19234.
  - [53] I. N. A. Khairil Anuar, A. Banerjee, A. H. Keeble, A. Carella, G. I. Nikov, M. Howarth, *Nat. Commun.* **2019**, *10*, 1–13.
  - [54] T. J. Powell, J. D. Silk, J. Sharps, E. Fodor, A. R. M. Townsend, *J. Virol.* **2012**, *86*, 13397–13406.
  - [55] J. Xiao, P. Rijal, L. Schimanski, A. K. Tharkeshwar, E. Wright, W. Annaert, A. Townsend, *J. Virol.* **2017**, *92*, e00941-17.
  - [56] P. Rijal, B. B. Wang, T. K. Tan, L. Schimanski, P. Janesch, T. Dong, J. W. McCauley, R. S. Daniels, A. R. Townsend, K.-Y. A. Huang, *J. Virol.* **2020**, *94*, e01182-19.
  - [57] Y. Hsia, J. B. Bale, S. Gonen, D. Shi, W. Sheffler, K. K. Fong, U. Nattermann, C. Xu, P.-S. Huang, R. Ravichandran, S. Yi, T. N. Davis, T. Gonen, N. P. King, D. Baker, *Nature* **2016**, *535*, 136–139.